The Isolation and Characterization of *Staphylococcus epidermidis* Bacteriophages for Phage Therapy Use

Emily Wood

A Thesis Submitted to the University of Ottawa in Partial Fulfillment of the Requirements for the Degree of Master of Science, Microbiology and Immunology

Department of Biochemistry, Microbiology, and Immunology

Faculty of Medicine

University of Ottawa

Abstract

Medical device-associated infections are among the most common hospital-acquired infections, representing a major challenge in modern healthcare. Periprosthetic joint infections (PJIs), occurring after joint replacements, are a common and particularly destructive infection, with more than 50% caused by *Staphylococcus* species. *Staphylococcus epidermidis*, a frequent culprit, is an opportunistic pathogen normally found on the skin, that becomes infectious when it colonizes implanted medical devices within the body. Unlike other *Staphylococcus* species, biofilm formation is the primary virulence factor of *S. epidermidis* in infections. Biofilms are complex structural communities that evade host-immunity and antibiotics. Rising antimicrobial resistance and the resistant nature of bacterial biofilms highlights an urgent need for alternative treatments, with phage therapy emerging as a promising solution. Bacteriophages (phages) are viruses that infect bacteria, and are incredibly abundant in nearly every environmental niche, including the human skin microbiome. However, phages are highly specific, and therapeutic use relies on access to large, diverse libraries to find effective matches against clinical isolates. Among 206 phages reported in literature to infect coagulase-negative *Staphylococci*, only 82 target *S. epidermidis*. This study aims to expand the availability of *S. epidermidis* bacteriophages by generating a biorepository with potential for phage therapy use.

Since May 2024, in conjunction with the TMM Bacteriophage Discovery Lab course, we have isolated nearly 100 phages from human skin swab samples against 7 *S. epidermidis* and 1 *S. succinus* strain, with 64 phages having been archived and implemented into this collection. Phages were genomically characterized by Oxford Nanopore long-read sequencing, with preliminary results demonstrating genomic diversity within our collection among 3 distinct clusters. To identify therapeutic candidates, we have evaluated host range infectivity, lytic efficiency against

planktonic bacterial growth, and anti-biofilm activity among a promising subset of lytic phages. This work will contribute to production of an Ottawa-based phage biorepository intended to improve access and efficiency for future emergent phage therapy cases.

Acknowledgements

I would like to express my gratitude to Dr. Adam Rudner for his unwavering support and guidance over the past three years. I would not be where I am today without your willingness to take me on as an undergraduate student. Thank you for trusting me to take on this project– it has become something I am incredibly passionate about.

Thank you to Dr. Liz Williams for your constant support throughout my time in the lab. I truly appreciate always being able to turn to you to discuss and troubleshoot my ideas and concerns.

Thank you to Celina Tanbari, Sunny Sun, and Ali Issa, for your contributions in all facets of this project and to Kieran Furlong for your expertise with genome sequencing. This study would not have been possible without each of you.

To my fellow lab members, thank you for always being there to talk about everything, both lab-related and not– you each made the lab such an enjoyable place to be.

I am so grateful to my family and friends who have supported me throughout my education. Thank you to everyone who has made Ottawa feel like home, and to my family back home who have consistently encouraged me from afar. To my mother, Priya Wood, I would not be where I am today without your sacrifice and support.

Statement of Contributions

Aims of this project were established by Emily Wood and Dr. Adam Rudner.

Phage isolation protocol was optimized by Emily Wood and carried out by Emily Wood, Celina Tanbari, and TMM3009 students.

TEM imaging was carried out by Emily Wood, Celina Tanbari, Katie Dale, Emma Pothier, TMM3009 students, and Dr. Adam Rudner.

Direct-from-plaque nanopore sequencing protocol was developed by Dr. Patrick Lypaczewski and Brenna Fox, optimized by Kieran Furlong, Celina Tanbari, and Adam Rudner, and carried out by Kieran Furlong, Celina Tanbari, Emily Wood, and TMM3009 students. Genome clustering and phylogeny determinations were carried out by Emily Wood.

Host Range assays were performed by Emily Wood, Celina Tanbari, and TMM3009 students.

Growth Curve assays were developed, optimized, and carried out by Emily Wood.

Biofilm assays were developed, optimized, and carried out by Emily Wood.

Table of Contents

List of Tables

List of Figures

Chapter 3 – Results

3.1 – Establish and Optimize Protocols for Work with Phages Infecting *S. epidermidis*

3.2 – Genomic Characterization of *Staphylococci* Bacteriophages

3.3 – Characterization of *Staphylococci* Bacteriophages for Phage Therapy

List of Abbreviations

A
agr – accessory gene regulator
AMMI – association of medical microbiology and infectious disease Canada
AMP – antimicrobial peptides
AMR – antimicrobial resistance
AT – adenine-thymine

B
Bp – base pair

C
CFU – colony forming units
CoNS – coagulase negative *Staphylococci*
CV – crystal violet

D
DNA – deoxyribonucleic acid
Ds – double stranded

E
ECM – extracellular matrix
EDTA – ethylenediaminetetraacetic acid
eDNA – extracellular DNA
EOL – efficiency of lysogeny
EPS – exopolysaccharides

F
Fg – fibrinogen

I
ICTV – international committee on taxonomy of viruses

M
MDAI – medical device associated infections
MDR – multi-drug resistant
MOI – multiplicity of infection
MRSE – methicillin-resistant *Staphylococcus epidermidis*
MSCRAMM – microbial surface components recognizing adhesive matrix molecules

N
NCBI – national center for biotechnology information

O
OD – optical density

P
PB – phage buffer
PEG – polyethylene glycol
PFU – plaque forming unit
Phage – bacteriophage
PhageSTAR – phage science therapeutics and research
PIA – polysaccharide intercellular adhesin
PJI – periprosthetic joint infection
PT – phage therapy

R
RBP – receptor binding protein

T
TEM – transmission electron microscopy
THA – total hip arthroplasty
TKA – total knee arthroplasty
TGY – tryptone glucose yeast extract media
TSB – tryptic soy broth media

Chapter 1 – Introduction

In February 2024, Infectious Disease Physician-Scientist of The Ottawa Hospital, Dr. Marisa Azad, was faced with the heart-breaking case of a 79–year–old woman presenting with a devastating infection of her artificial hip implant. The patient, Ms. Thea Turcotte, had undergone 15 major revision surgeries, numerous rounds of antibiotics, and had ultimately developed sepsis. The cause? The implant had been colonized by the bacterium *Staphylococcus epidermidis*, and infection had rampantly spread through the body. With conventional treatment options exhausted, Dr. Azad turned to phage therapy– an experimental treatment utilizing bacteriophages, viruses that kill bacteria, to fight antibiotic resistant infections (1, 2).

1.1 – Periprosthetic Joint Infections

Infections associated with implanted medical devices represent a major challenge in modern healthcare, often leading to devastating complications and extended hospitalizations (3). Ms. Turcotte's condition, a periprosthetic joint infection (PJI), represents a particularly destructive implant associated infection. PJIs are a complication of joint arthroplasties, surgeries where artificial implants are used to restore function in damaged joints (4). These surgeries most commonly include total hip arthroplasty (THA) and total knee arthroplasty (TKA), with the most frequent indications being osteoarthritis or femoral neck fractures and most often occurring in older populations (5). As medical technology improves and demand rises, incidence of these procedures increases, with more than 175,000 hip and knee replacements occurring in Canada in 2024–2025, a 26% increase from 2019–2020 (6). PJIs occur in roughly 1–2% of joint arthroplasties, most often occurring 4–weeks to 2–years following the primary surgery (4). A Canadian study of 129,613 TKA patients aged 50 or older described PJI incidence of 0.51% at 1–year post-operation, increasing to 1.65% at 15–years post-operation (7). These post-surgical

infections may be caused by a wide range of bacteria, and fungi in some cases, and occur when pathogens infiltrate and infect the area surrounding an artificial joint (4).

1.2 – *Staphylococcus epidermidis*, The Opportunistic Pathogen

Staphylococcal species, and in particular *Staphylococcus epidermidis*, are responsible for more than 50% of hip and knee PJIs (8). *S. epidermidis*, formerly *S. albus*, is a gram-positive cocci bacterium of the phylum Bacillota and *Staphylococcus* genus (9). It was first distinguished from the more commonly known *Staphylococcal* species *S. aureus*, by the opaque white colour of its colonies by microbiologist Friedrich Julius Rosenbach in 1884 (9). *S. epidermidis* is a facultative anaerobe, with an optimal growth temperature between 30ºC–37ºC. *S. epidermidis* is classified as a coagulase-negative *Staphylococcal* (CoNS) species, a distinction used to classify *Staphylococci* which do not produce coagulase, an enzyme aiding in blood clotting; *S. epidermidis* is the leading CoNS associated with PJIs (10).

As implied by its name, *S. epidermidis* inhabits epithelial tissues, particularly at the level of the stratum corneum, and is the most abundant bacteria found on skin and mucous membranes in the human body, with key roles in maintaining skin homeostasis and stimulating immune activity (11, 12). It resides naturally as a commensal among the topical human skin flora, predominantly abundant in moist and sebaceous areas such as the axilla, nasal cavity, antecubital and popliteal creases, and plantar surfaces (13). *S. epidermidis* plays a crucial role in its dynamics with other skin commensals, including *Cutibacterium acnes*, where *S. epidermidis* may keep the acne-causing bacterium at bay through glycerol fermentation, and *C. acnes* adjusts pH to reduce *Staphylococcal* growth (13). *S. epidermidis* may also modulate the skin homeostasis through secretion of sphingomyelinase, a key molecule which breaks down sphingomyelin on the skin, producing ceramides; important molecules in maintaining skin elasticity and barrier (14).

Commensal *S. epidermidis* also plays a key role in wound healing and infection defense, primarily through preventing colonization from pathogens, including *Staphylococcus aureu*s. These effects primarily occur through release of antimicrobial compounds, disruption of biofilm, and modulation of the hosts immune system (15).

S. epidermidis is generally described as an opportunistic pathogen, while it remains harmless in its natural environment as a commensal on the skin microbiota, it may become pathogenic when given the opportunity to colonize surfaces of foreign implants. Once introduced inside the body, most often during the surgical process, *S. epidermidis* can rapidly spread through the bloodstream, creating major complications which are incredibly difficult to treat (11). *S. epidermidis* is responsible for a broad assortment of medical device associated infections (MDAI), including PJIs, catheter-related bloodstream infections, prosthetic valve endocarditis, central nervous system shunt infections, and infection of cardiac devices, breast implants, and ocular implants. This bacterium rarely causes infection of native tissue without involvement of a foreign body (16).

1.3 –Biofilm Formation by *Staphylococcus epidermidis*

Biofilm formation is the predominant virulence factor associated with pathogenicity of *S. epidermidis* (17). Bacterial biofilms are communities of bacteria which arrange into robust structures and harbour unique physical and chemical characteristics that protect bacteria against antibiotics and host immune system defences (18). *S. epidermidis* biofilm formation is characterized into four key steps: adherence, accumulation, maturation, and dispersal (17).

1. **Adherence.** Biofilm formation begins with attachment of the bacterium to biotic or abiotic surfaces found inside the body, most commonly including implanted biomaterials such as catheters and prosthetics. This infiltration of foreign devices occurs largely due to ease of binding to the adhesion medium present on these devices, often containing human body

fluids and proteins including fibronectin, fibrinogen (Fg), and albumin, present to support integration of the implant into the body tissue (16). *Staphylococci* species frequently encode multiple Microbial Surface Components Recognizing Adhesive Matrix Molecules (MSCRAMMs), which support binding to adhesion proteins, or nonspecific binding through hydrophobic interactions (17, 19, 20). Many *S. epidermidis* isolates encode the SdrG protein, a cell-surface adhesin protein which binds Fg-coated biomaterials (21).

2. **Accumulation**. Production of the biofilm extracellular matrix (ECM) represents the start of the accumulation phase. The ECM is a slimy, heterogenous structure, primarily composed of exopolysaccharides (EPS), in addition to extracellular DNA (eDNA), lipids, and proteins, all self-synthesized by the bacterium (19). Polysaccharide intercellular adhesin (PIA), first described by Mack and colleagues in 1996, is a common EPS amongst *Staphylococci* species, and is the major EPS formed by *S. epidermidis* (19, 22). PIA facilitates intercellular adhesion amongst *Staphylococcal* cells in the ECM, forming a fibrous 'net' which supports structural integrity of the biofilm and resistance to mechanical strains (17, 19).

   PIA is encoded by the *icaADBC* locus, a highly conserved sequence with a diverse array of homologues among other biofilm forming bacteria, including the *pgaADBC* operon in *Escherichia coli* (19). The *icaADBC* locus consists of an *icaR* repressor region upstream of the *icaADBC* operon, which halts expression of these genes dependent on varied environmental conditions (17, 19). The *icaA* and *icaD* protein products are membrane proteins which synthesize the PIA chain, *icaC* is responsible for export of the PIA chain through the cytoplasmic membrane, and *icaB* produced a deacetylase, which adds positive charge on the biofilm surface promoting adherence of the biofilm to the cell surface (17,

19). However, *S. epidermidis* biofilm formation has been found in *ica*$^{-}$ mutants, primarily through function of alternative surface adhesion proteins (20).

3. **Maturation**. PIA is heavily involved in biofilm maturation, as a robust three-dimensional tower structure is generated through cell accumulation. As the structure grows, layers with different metabolic conditions emerge, where young layers at the upper region of the biofilm are exposed to oxygen and glucose, but mature layers closer to the attachment site are limited of oxygen and have greater reliance on secondary carbon sources such as amino acids and peptides (17). The physical shield produced by a PIA-rich biofilm ECM supports *S. epidermidis* evasion of environmental stressors and the immune system, demonstrating resistance to phagocytosis by the innate immune system, antimicrobial peptides (AMPs), and antibiotics (19).
4. **Dispersal**. As the biofilm matures, individual cells or pieces of biofilm may detach and travel throughout the body to colonize new surfaces– this is the key mechanism of expanding infection (17). The detachment process is mediated by an accessory gene regulator (*agr*), a quorum-sensing network active at the biofilm surface, which may destroy EPS enzymatically or by disruption of noncovalent interactions (17, 20). This detachment process is a leading cause of *S. epidermidis* bloodstream infections, with sepsis and septic shock as detrimental complications (11).

The molecules involved in formation of *S. epidermidis* biofilms are highly varied among strains, and their mechanisms of maturation and dispersal are greatly undiscovered. As a result, *S. epidermidis* PJIs are notoriously difficult to treat due to biofilm formation and the resistant nature of biofilms against antibiotics and immune cells (23). *S. epidermidis* biofilms in PJI are most commonly monomicrobial, however they may be involved in polymicrobial biofilms with other

bacteria or fungi, commonly including *Staphylococcus aureus*, *Enterococcus faecalis,* and *Candida albicans*, increasing overall pathogenicity of these infections (10).

1.4 – The Epidemic of Antimicrobial Resistance

Another layer of complication is added to these difficult-to-treat infections by the increasing incidence of antimicrobial resistance (AMR) among pathogens. AMR is an evolutionary feature of bacteria adapting their defence systems to survive, making treatment with common antibiotics increasingly difficult. This global crisis has become a leading cause of treatment failure, with an estimated 1.27 million deaths worldwide directly attributed to AMR in 2019 alone (24). Further, the World Health Organization and the United Nations have both identified AMR to be one of the top threats to global health, food security, and development. Studies have predicted that by 2050, antibiotic resistance will be responsible for more than 10-million deaths per year, surpassing cancer as a leading cause of death (25). Resistance is of particular concern for clinical cases of *S. epidermidis* infection, as 90% of clinical isolates are resistant to methicillin (MRSE) (26). As population-wide lifestyle changes contribute to increased disease states, and medical device technology advance, incidence of MDAIs is rising; and threat of associated bacterial infections poses even greater concern to healthcare providers and patients. As traditional antibiotic treatments struggle to keep pace with evolving multi-drug-resistant (MDR) pathogens, the search for alternative treatments has become more urgent. Bacteriophage therapy has emerged as a promising and innovative solution to the AMR crisis.

1.5 – Bacteriophages

Bacteriophages or ‘phages’ are viruses that are the natural predator of bacteria, estimated to have co-evolved with bacteria for nearly 44-billion years (27). They can selectively target and infect specific bacterial hosts, hijacking their biosynthetic machinery, and ultimately lysing them

as a result of their replication (28). Bacteriophages were first discovered in 1915 by Frederick Twort and named by Felix d'Herelle after his independent discovery in 1917 (28). Estimates suggest 10^{31} bacteriophages exist, classifying them as the most abundant biological entity on Earth (27). Phages are ubiquitous in nature, found in every ecological niche where bacteria are found, including oceans, lakes, soil, the gut microbiome, and human skin (27).

Bacteriophage infection follows 4 distinct steps: absorption, attachment, penetration, and phage infection cycle.

1. **Adsorption.** The mechanism by which phages identify and target a potential host, predominantly driven by the tail structure. Diffusion and Brownian motion are the primary mechanisms through which a phage may randomly find a bacterial host in space (29). This process allows the phage to collide with a particular host receptor.
2. **Attachment**. Unique receptor binding proteins (RBP) located at the distal end of the tail allow bacteriophages to recognize and infect their bacterial host. RBPs identify specific combinations of molecular structures on the bacterial cell wall, flagella, or pili, typically wall teichoic acids among *Staphylococci* phages, which serve as the common binding site (30). This feature is the hallmark of the diversity and specificity of bacteriophages to their host, as each phage displays a slightly different combination of RBPs complementary to different surface receptors– resulting in varying ability among phages to infect different *S. epidermidis* species (30). When recognized, RBPs interact in a reversible primary interaction, followed by an irreversible secondary interaction, with the same or a new receptor (29). During this stage, some phages may also use tail-assisted depolymerases to degrade protective components surrounding the bacterial cell wall, including EPS, to support the phage reaching the bacterial receptor. Many phages infecting *S. epidermidis* have been found to encode depolymerases (29).

3. **Penetration.** Completion of the irreversible secondary interaction triggers ejection of the bacteriophage genome. This process differs among two distinct structural types of tailed bacteriophages.
    a. **Contractile Tailed.** In contractile phages of the *Myovirus* morphotype, penetration occurs through a syringe mechanism. This is facilitated by disruption of the baseplate, and contraction of the inner sheath through the bacterial cell wall to push the genome through the tail tube into the bacterial cell.
    b. **Non-Contractile Tailed.** In non-contractile phages of the *Siphovirus* and *Podovirus* morphotype, genome transfer occurs with passive transport through the tail tube, where depolymerase enzymes are used to degrade the bacterial cell wall.

    The genome is injected into the bacterium, and the phage infection cycle begins.

4. **Infection Cycle.** Following penetration, bacteriophages may undergo one of two life cycles which they utilize to maximize their infectibility and survival.
    a. **Lytic cycle**. Virulent phages enter the lytic cycle and are ultimately bacterial killers. The genome is injected into the host cell cytoplasm where it becomes circularized into its replicative form, allowing stability and preventing degradation by some host nucleases. The phage then hijacks the host's replication and translation machinery, that are then utilized to replicate its genome and produce phage proteins (28). New virions are self-assembled and accumulate, and lytic proteins begin to degrade the cell wall, eventually causing the host to lyse, releasing more phage (28).
    b. **Lysogenic cycle**. Temperate phages hide their genomes within the bacterial genome. After injection, the genome is integrated into the bacterial genome, creating a "prophage" (28). Prophages allow for phage genomes to replicate inside the bacterial

cell through cell division. In some cases, prophages may benefit their host, serving as a mechanism for the transmission of antibiotic resistance to the host through transduction. Particularly of concern are phages encoding genes which are distinctive of lysogeny, virulence factors, and AMR (28). The lysogenic cycle typically occurs in high nutrient conditions, but when the host cell experiences stress, in the form of starvation or DNA damage, the prophage may be "induced" and recombine out of the genome and re-enter the lytic cycle. The regulation of the lytic/lysogenic switch has been extensively studied in several *E. coli* phages and relies on a transcription factor, the immunity repressor, that maintains lysogeny by promote its own expression and represses the expression of early lytic genes (31). In most populations of lysogens, an equilibrium exists between cells that maintain and induce their prophage. Many *S. epidermidis* strains are known to contain one or multiple prophages within them, with those prevalent in clinical strains offering potential for horizontal transfer and transduction of resistance and pathogenicity genes, promoting virulence of the pathogenic bacteria (26).

1.6 – Bacteriophages Infecting *Staphylococci*

All known bacteriophages infecting *S. epidermidis* are of the order *Caudovirales*, designating tailed phages which contain double stranded (ds) deoxyribonucleic acid (DNA) genomes (32). Phage genomes largely mirror the nucleotide content of their hosts; *S. epidermidis* is largely Adenine-Thymine (AT) rich, thus, most *S. epidermidis* phages exhibit AT rich content (16). Viruses of the order *Caudovirales* were previously organized based on morphological family, which included *Myoviridae*, *Siphoviridae*, and *Podoviridae*, where all three members contain an icosahedral capsid which houses the ds DNA genome; and a contractile, long non-contractile, and

short non-contractile tail, respectfully (32). The International Committee on Taxonomy of Viruses (ICTV) has recently shifted classification of *Staphylococci* phages to be based on nucleotide similarity, where the above-mentioned organization is only used to describe virus morphology (33).

For the purposes of this thesis, phages are organized into 4 distinct clusters (A-D) based on a 2019 paper by Oliveira and colleagues (34). This organization uses a pairwise shared gene content clustering method, with a threshold of 35% similarity (34).

Cluster A – Podoviruses within the *Roundtreeviridae* family. Oliveira and colleagues described 16 distinct phages within this category, falling into two subclusters (A1, A2), with two *S. epidermidis* bacteriophages falling under A2 (St134, Andhra) (34). Phages within this cluster have well-conserved features including a 16-18kB genome encoding 20-22 proteins with about 60% of known function (34). These phages are not found to encode lysogenic genes and follow a lytic lifestyle.

Cluster B – Siphoviruses within an unclassified *Siphoviridae* family. Oliveira and colleagues described 132 distinct phages within this category, falling into seventeen subclusters (B1-B17), with five and one *S. epidermidis* bacteriophages falling under B4 (vB_SepiS-philPLA5, vB_SepiS-philPLA7, PH15, etc.) and B13 (StB20-like), respectively (34). Phages within this cluster are quite diverse with genomes sizes varying 39-48kB encoding 42-79 proteins with <50% of known function (34). Most contain lysogenic genes including the integrase and repressor, maintaining their temperate lifestyle and ability to form prophages host. The integration system may feature either as a serine or tyrosine integrase from one of five phams and is not specific to subcluster or host species (34). Additional phages in Cluster B have since been discovered to lack an integrase and instead undergo their

lysogenic functionality through transduction (Sazerac) (35). Additionally, virulence genes exist exclusively in some subclusters of Cluster B phages, however notably none have been identified in subcluster B4 or B13 phages (34). Due to their lysogenic capabilities and ability to transmit virulence to their host, phages of Cluster B are not permitted for use in phage therapy.

Cluster C – Myoviruses within the *Herelleviridae* family. Oliveira and colleagues described 53 distinct phages within this category, falling into six subclusters (C1-C6), with five *S. epidermidis* bacteriophages falling under C3 (philBB-SEP1, Terranova, Quidividi, Twillingate) (34). Phages within this cluster have well-conserved features including a 127-151kB genome encoding 164-249 proteins with <40% of known function (34). These genomes are characterized by direct terminal repeats, reflecting their large genome size. Notably, Subclusters C3, C4, and C5 share <60% of their genes with other Cluster C phages and may infect rarer serotypes of host species (34). These phages are not found to encode lysogenic genes and are described to have a broader host range (34).

Cluster D – Siphoviruses within an unclassified *Siphoviridae* family of the Subfamily *Sextaecvirus.* Oliveira and colleagues described 3 distinct phages within this category, falling into two subclusters (D1, D2), with two *S. epidermidis* bacteriophages falling under D1 (6ec, vB_SepS-SEP9) (34). Phages within this cluster have an 89-93kB genome, encoding 129-142 proteins with ~35% of known function (34). Cluster D phages are not found to encode lysogenic genes. Additionally, these viruses differ morphologically from Cluster B Siphoviruses, often having a much longer (>300nm) flexible tail (34).

Singleton – Siphovirus SPbeta-like within a singleton family. Oliveira and colleagues described 1 distinct *S. epidermidis* phage in a singleton family. SPbeta-like has a 127kB

genome, encoding 177 genes with <30% of known function (34). SPbeta-like is not found to encode lysogenic genes and shares <10% gene content with other *Staphylococcal* phages (34).

1.7 – Phage Therapy

As previously described, the therapeutic use of bacteriophages against bacterial infections is delineated "phage therapy" (PT) (28). While PT is seeing a recent resurgence in the Western world, this therapy has existed for over a century and was used successfully long before the discovery of antibiotics. The first documented case of clinical PT was pioneered by Felix d'Herelle in 1919 at the Hôpital des Enfants-Malades in Paris as treatment against a case of pediatric bacterial dysentery (28). Since then, PT has been used clinically for nearly a century, having been maintained as a common treatment in the former Soviet Union and many Warsaw-pact counties, but fell out in the West in the discovery of antibiotics due to their wide-range effects and commercialization (28). As AMR rises and antibiotic treatments become obsolete against many pathogens, PT is being rediscovered for compassionate use cases, and for many patients has demonstrated great success and little-to-no toxicity (36, 37).

While PT is not currently a licensed treatment in Canada, single patient trials for PT use as an investigational new drug have been considered for patients with infections not responding to antibiotics. The first use of PT in Canada occurred in 2023 at the St. Josephs Health Centre in Toronto for a drug-resistant urinary tract infection caused by *E. coli* (38). Since 2023, PT has been used only a handful of times, including the treatment of Ms. Turcotte's infection, which marked the first use of PT for a PJI in Canada (1). Canadian phage research is being supported through the Phage Science Therapeutics and Research (PhageSTAR) program in collaboration with the Association of Medical Microbiology and Infectious Disease Canada (AMMI) and Health Canada, with aims to develop clinical and regulatory guidelines for PT by 2028 (39).

Guidelines for phage therapy use are more developed in other countries, with several guidelines governing the selection of a particular therapeutic phage (27, 37).

1. Phages considered for therapy must be extensively characterized *in vitro* through an in depth whole-genome sequence analysis to ensure the genome does not contain any genes encoding AMR or toxins. These factors might be spread via transduction to the pathogen, offering deleterious effects.
2. Lytic phages are required for phage therapy as they limit risk of prophage formation, which may act a vector to spread AMR. This may be assessed in a genome sequence, searching for genetic elements indicative of lysogeny (i.e. the integrase) as well as observation of transduction capabilities. Thus, phages of cluster A, C, and D contain phages that may be suitable for phage therapy, while phages of cluster B should not be used (34).
3. Phages must demonstrate host specificity to a particular pathogenic strain, and an ability to kill that host efficiently.
4. It must be possible to generate and maintain a stable concentration of this phage.
5. Phages must be pure, free of contamination from the host, or harmful toxins.

1.7 – The Bottleneck

The major bottleneck to efficient deployment of PT as an emergency therapeutic, or eventual common treatment, remains to be the availability of therapeutic phages, and the specificity of phages to their host. All PT success hinges on finding phages which infect a particular infection-causing strain. Limitations are created by the narrow availability of specific collections for phages infecting human pathogens. A limited number of bacteriophages infecting *S. epidermidis* species have been isolated, and even fewer have been fully characterized *in vitro*. The 2019 study by Oliveira and colleagues highlighted one of few *Staphylococcal* phage collections, where of 205 *Staphylococcal* phages, only 16 phages infected *S. epidermidis* (34). A 2025 review by Lopes and

colleagues analyzed all 206 CoNS phages among several independent collections and GenBank available as of February 2023, of which 40% (n=82) infected *S. epidermidis* (40, 34). This study, being the largest review of *Staphylococcal* phages available to-date, highlights the 82 *S. epidermidis* bacteriophages that are available for potential therapeutic use. This current availability pales in comparison to Actinobacteriophage collections, where nearly 10,000 phages capable of infecting *Mycobacterium smegmatis* have been isolated (41).

Staphylococcal phages exhibit a high degree of specificity, with each phage often targeting a particular species or strain within a genus. With such narrow specificity observed among these bacteriophages, broad collections are the primary way to ensure that a successful phage can be found for a particular infection-causing strain.

1.8 – Objectives

This study aims to create a diverse and well-characterized library of bacteriophages infecting *S. epidermidis* to contribute to existing biorepositories of *Staphylococci* phages, with the intention of availability for use in future PT cases. This work will improve access to therapeutic phages, thereby reducing the major bottlenecks to deployment of PT and supporting efforts for PT to become a more widely used treatment option in Canada.

1.9 – Aims

The goals of this Master's project are outlined in three specific aims:

1. Create a diverse collection of *S. epidermidis* phages.
2. Genomic characterization of *Staphylococci* bacteriophages.
3. Characterization of *Staphylococci* bacteriophages for phage therapy.

Chapter 2 – Materials and Methods

2.1 – Culturing Strains

Frozen stock of *S. epidermidis* strains were struck on Tryptone Glucose Yeast (TGY) plates and grown for 24–36 hours at 34ºC. Colonies were inoculated into TGY media and grown under continuous orbital shaking at 210 rpm at 34ºC. Cultures were grown to saturation and transferred to room temperature for use up to 2–weeks.

Note: Due to slight variation in indicated isolation temperatures between strains in the collection ranging from 28ºC–37ºC, we chose to grow all strains in the collection at 34ºC. Additionally, growth in TSB was more optimal for some bacteriophages and/or experimental conditions (i.e. biofilm experiments), thus was used in lieu of TGY in these cases,

Table 1. *Staphylococcus* Host Strains. 13 different *S. epidermidis* strains and 1 *S. succinus* strain were sourced from NRRL and ATCC for use in this project.

Species	ID	Source	Risk Group
S. epidermidis	NRRL 41021	Laboratory Pig Epidermis	BSL 1
S. epidermidis	NRRL 41571	Ground Beef	BSL 1
S. epidermidis	NRRL 41570	Ground Beef	BSL 1
S. epidermidis	NRRL 41129	Ground Turkey	BSL 1
S. epidermidis	NRRL 41142	Ground Beef	BSL 1
S. epidermidis	NRRL 41574	Tapioca Pudding	BSL 1
S. epidermidis	NRRL 41251	Beer	BSL 1
S. epidermidis	NRRL 41575	Tapioca Pudding	BSL 1
S. epidermidis	NRRL 41253	Beer	BSL 1
S. epidermidis	NRRL 41577	Ground Turkey	BSL 1
S. epidermidis	NRRL 4268	N/A	BSL 1
S. epidermidis	NRRL 2616	N/A	BSL 1
S. epidermidis	ATCC 35984	Clinical Isolate: Catheter Sepsis	BSL 1
S. succinus	ATCC 700337 (DMZ 14617)	Plant and Soil Inclusions with 25–35-Million-Year-Old Amber	BSL 1

2.2 – Phage Isolation from Skin Swab Samples

The direct isolation workflow for isolation of these bacteriophages was adapted from the SEA–PHAGES Discovery Guide and the 2021 study by Valente & colleagues (42, 43). Ethical considerations of the volunteer sampling method and the ownership of the phages was approved by the University of Ottawa Faculty of Medicine Research Ethics Board (protocol # H-06-24-10454) and has been implemented for use by students in the University of Ottawa Faculty of Medicine's TMM3009 course and public volunteers by the Rudner Laboratory.

Samples were self–collected by healthy volunteers: cotton pads were dampened slightly with water and rubbed vigorously on the skin for 30 seconds, sampling locations varied and successful locations commonly included underarms, nostrils, forehead, back, and feet. Swabs were deposited into conical tubes and stored at room temperature or 4ºC for ≤24 hours. TGY media was added into conical tubes to saturate swabs (5–10 mL), samples were shaken at 210 rpm and 34ºC for 2 hours, 500 μL of sample was removed and filtered through a 0.22 μm filter. 500 μL of filtrate was incubated with 250 μL of an *S. epidermidis* culture for 10 minutes and plated on TGY plates with 4.5 mL of TGY top agar using the double agar overlay method (42). Plates are incubated at 34ºC overnight and observed for clearings (plaques) in the *S. epidermidis* lawn indicating phage presence (43).

2.3 – Purification of Phage Sample

Isolated plaques were picked with a sterile pipette tip through the top layer of agar and inoculated into phage buffer (PB). Phage suspension was serially diluted through 1:10 dilutions in PB from 10^{-1} to 10^{-5}, and 100 μL of each dilution was plated on a TGY plates following the same method as above. This process was repeated 1–2 more times to ensure purified phage sample.

2.4 – Phage Amplification on Plates

Dilutions of phage suspension were plated with TGY agar and incubated at 34ºC overnight. Plates with sufficient "webbing" (those with majority of the lawn cleared by phage) were flooded with phage buffer (PB). Flooded plates were incubated overnight to release phage into buffer and suspension (lysate) was collected and filter sterilized through 0.22 μm filters. Spot assays were performed as described below and repeated with different bracketing of phage concentration if necessary.

2.5 – Phage Amplification in Liquid

1 mL of *S. epidermidis* strain was inoculated into three 150 mL flasks, each containing 25 mL TGY media. Varying concentrations of phage were added (0.2x, 1x, 5x the amount expected to form a webbed plate). Contents of the flasks were swirled and incubated at room temperature for 20 minutes. Flasks were placed at 220 rpm at 34ºC for 16-18 hours, or until clearing was observed. Samples were centrifuged at 4000 rpm for 5 minutes and supernatant was filtered through 0.22 μm filter. Note: high titer lysate can be obtained from cultures despite not having visually cleared.

2.6 – Phage Titering

To calculate the concentration of phage, lysates were serially diluted 1:10 in phage buffer and 3–5 μL of each dilution were spotted on TGY plates. Plates were grown at 34º overnight and the PFU was calculated based on the presence of plaques using the following equation: $Titer\left(\frac{pfu}{mL}\right) = \frac{\#\ plaque\ forming\ units}{volume\ of\ phage}\ x\ \frac{1}{dilution\ factor}$. Lysates with a calculated titer of >1x10^9 pfu/mL were considered "high titer" and may be archived for the collection.

2.7 – Archiving Phage

940 μL of purified and filtered high titer lysates were mixed with 60 μL of DMSO and stored at –80ºC. Additional lysate without DMSO was stored at 4ºC.

2.8 – Direct–from–plaque Nanopore Sequencing

Samples containing phage DNA were collected by sterile picking of a well–isolated plaque formed by a bacteriophage on a TGY agar plate with a *S. epidermidis* lawn. Samples were suspended in 50 µL TE buffer, briefly vortexed, and heated at 65ºC for 10 minutes. 2.25 µL of TE sample were transferred to a chilled PCR tube and mixed with 0.75 µL MuA transposase. Samples were flicked to mix, briefly spun down, and transferred to a thermocycler and the following cycle was run: 2 minutes at 4ºC, 2 minutes at 30ºC, 2 minutes at 80ºC, and held at 4ºC, to allow insertion, activation, and inactivation of the transposon, "tagmentation". 0.5 µL of tagmented DNA was mixed in a PCR tube containing 10 µL SuperFi master mix, 4 µL of 2.5 µM barcoded oligo, and 5.5µL nuclease–free water. Tubes were transferred to a thermocycler, and the following PCR cycle was run: (10 minutes at 98ºC, 10 minutes at 60ºC, 5 minutes at 72ºC) x 30, 5 minutes at 72ºC, and held at 4ºC. 5 µL of amplified and barcoded DNA was run on 1% agarose gel in 1X TAE to assess amplification and quality of fragmentation. Multiple barcoded samples (up to 96) were pooled and balanced. Rapid adaptors were attached through click chemistry to a moiety present on the barcoded oligo. Genomic DNA was sequenced on an ONT Minion R10.4.1 chemistry. Reads were assembled and analyzed by NCBI Nucleotide Blast to assess similarity to existing *S. epidermidis* bacteriophages. This protocol was adapted from Brenna Fox and Patrick Lypaczewski from McGill University (44). FASTA files of genome sequences were organized by PhageScope and a phylogenetic tree was created through Interactive Tree of Life (iTol) software (45, 46).

Supplementary Table 1. Table of Nanopore Barcodes. 96 distinct barcoded sequences were utilized in preparation of the Nanopore sequencing library. Table denotes universal sequence, unique barcoded sequence, and target primer.

well	tag	universal (M13F)	barcode	target primer	well	tag	universal (M13F)	barcode	target primer
A1	27f_PL001	GTA AAA CGA CGG CCA GTG	aaaacgaa	CGTTTTTCGTGCGCCGCTTC	E2	27f_PL050	GTA AAA CGA CGG CCA GTG	ctacctca	CGTTTTTCGTGCGCCGCTTC
A2	27f_PL002	GTA AAA CGA CGG CCA GTG	aaaatatt	CGTTTTTCGTGCGCCGCTTC	E3	27f_PL051	GTA AAA CGA CGG CCA GTG	ctatggac	CGTTTTTCGTGCGCCGCTTC
A3	27f_PL003	GTA AAA CGA CGG CCA GTG	aaataaac	CGTTTTTCGTGCGCCGCTTC	E4	27f_PL052	GTA AAA CGA CGG CCA GTG	ctcgcacc	CGTTTTTCGTGCGCCGCTTC
A4	27f_PL004	GTA AAA CGA CGG CCA GTG	aaccatca	CGTTTTTCGTGCGCCGCTTC	E5	27f_PL053	GTA AAA CGA CGG CCA GTG	ctgtcaga	CGTTTTTCGTGCGCCGCTTC
A5	27f_PL005	GTA AAA CGA CGG CCA GTG	aagagtta	CGTTTTTCGTGCGCCGCTTC	E6	27f_PL054	GTA AAA CGA CGG CCA GTG	cttgataa	CGTTTTTCGTGCGCCGCTTC
A6	27f_PL006	GTA AAA CGA CGG CCA GTG	aagatgcg	CGTTTTTCGTGCGCCGCTTC	E7	27f_PL055	GTA AAA CGA CGG CCA GTG	gaacttac	CGTTTTTCGTGCGCCGCTTC
A7	27f_PL007	GTA AAA CGA CGG CCA GTG	acactgag	CGTTTTTCGTGCGCCGCTTC	E8	27f_PL056	GTA AAA CGA CGG CCA GTG	gaatcgcg	CGTTTTTCGTGCGCCGCTTC
A8	27f_PL008	GTA AAA CGA CGG CCA GTG	accgacaa	CGTTTTTCGTGCGCCGCTTC	E9	27f_PL057	GTA AAA CGA CGG CCA GTG	gacgcgta	CGTTTTTCGTGCGCCGCTTC
A9	27f_PL009	GTA AAA CGA CGG CCA GTG	accgctct	CGTTTTTCGTGCGCCGCTTC	E10	27f_PL058	GTA AAA CGA CGG CCA GTG	gacttccc	CGTTTTTCGTGCGCCGCTTC
A10	27f_PL010	GTA AAA CGA CGG CCA GTG	acgcccta	CGTTTTTCGTGCGCCGCTTC	E11	27f_PL059	GTA AAA CGA CGG CCA GTG	gaggcact	CGTTTTTCGTGCGCCGCTTC
A11	27f_PL011	GTA AAA CGA CGG CCA GTG	acgggaga	CGTTTTTCGTGCGCCGCTTC	E12	27f_PL060	GTA AAA CGA CGG CCA GTG	gataccac	CGTTTTTCGTGCGCCGCTTC
A12	27f_PL012	GTA AAA CGA CGG CCA GTG	acgtcaat	CGTTTTTCGTGCGCCGCTTC	F1	27f_PL061	GTA AAA CGA CGG CCA GTG	gattaaca	CGTTTTTCGTGCGCCGCTTC
B1	27f_PL013	GTA AAA CGA CGG CCA GTG	actatcct	CGTTTTTCGTGCGCCGCTTC	F2	27f_PL062	GTA AAA CGA CGG CCA GTG	gcaatgca	CGTTTTTCGTGCGCCGCTTC
B2	27f_PL014	GTA AAA CGA CGG CCA GTG	acttgtac	CGTTTTTCGTGCGCCGCTTC	F3	27f_PL063	GTA AAA CGA CGG CCA GTG	gcacagtc	CGTTTTTCGTGCGCCGCTTC
B3	27f_PL015	GTA AAA CGA CGG CCA GTG	agaacttc	CGTTTTTCGTGCGCCGCTTC	F4	27f_PL064	GTA AAA CGA CGG CCA GTG	gcattctg	CGTTTTTCGTGCGCCGCTTC
B4	27f_PL016	GTA AAA CGA CGG CCA GTG	agaggtag	CGTTTTTCGTGCGCCGCTTC	F5	27f_PL065	GTA AAA CGA CGG CCA GTG	gccgaatt	CGTTTTTCGTGCGCCGCTTC
B5	27f_PL017	GTA AAA CGA CGG CCA GTG	agatacgg	CGTTTTTCGTGCGCCGCTTC	F6	27f_PL066	GTA AAA CGA CGG CCA GTG	gccggggg	CGTTTTTCGTGCGCCGCTTC
B6	27f_PL018	GTA AAA CGA CGG CCA GTG	agccggga	CGTTTTTCGTGCGCCGCTTC	F7	27f_PL067	GTA AAA CGA CGG CCA GTG	gcctctag	CGTTTTTCGTGCGCCGCTTC
B7	27f_PL019	GTA AAA CGA CGG CCA GTG	agggtgaa	CGTTTTTCGTGCGCCGCTTC	F8	27f_PL068	GTA AAA CGA CGG CCA GTG	gctggcca	CGTTTTTCGTGCGCCGCTTC
B8	27f_PL020	GTA AAA CGA CGG CCA GTG	agtaagat	CGTTTTTCGTGCGCCGCTTC	F9	27f_PL069	GTA AAA CGA CGG CCA GTG	gcttccgt	CGTTTTTCGTGCGCCGCTTC
B9	27f_PL021	GTA AAA CGA CGG CCA GTG	agtcaatg	CGTTTTTCGTGCGCCGCTTC	F10	27f_PL070	GTA AAA CGA CGG CCA GTG	ggcactgt	CGTTTTTCGTGCGCCGCTTC
B10	27f_PL022	GTA AAA CGA CGG CCA GTG	agtttacc	CGTTTTTCGTGCGCCGCTTC	F11	27f_PL071	GTA AAA CGA CGG CCA GTG	ggcgatcc	CGTTTTTCGTGCGCCGCTTC
B11	27f_PL023	GTA AAA CGA CGG CCA GTG	atacgcct	CGTTTTTCGTGCGCCGCTTC	F12	27f_PL072	GTA AAA CGA CGG CCA GTG	ggcggaaa	CGTTTTTCGTGCGCCGCTTC
B12	27f_PL024	GTA AAA CGA CGG CCA GTG	atagattt	CGTTTTTCGTGCGCCGCTTC	G1	27f_PL073	GTA AAA CGA CGG CCA GTG	gggcagcg	CGTTTTTCGTGCGCCGCTTC
C1	27f_PL025	GTA AAA CGA CGG CCA GTG	atcaatag	CGTTTTTCGTGCGCCGCTTC	G2	27f_PL074	GTA AAA CGA CGG CCA GTG	ggtcgagc	CGTTTTTCGTGCGCCGCTTC
C2	27f_PL026	GTA AAA CGA CGG CCA GTG	atcgtgtg	CGTTTTTCGTGCGCCGCTTC	G3	27f_PL075	GTA AAA CGA CGG CCA GTG	gtatctgc	CGTTTTTCGTGCGCCGCTTC
C3	27f_PL027	GTA AAA CGA CGG CCA GTG	atgtgacg	CGTTTTTCGTGCGCCGCTTC	G4	27f_PL076	GTA AAA CGA CGG CCA GTG	gtcagcat	CGTTTTTCGTGCGCCGCTTC
C4	27f_PL028	GTA AAA CGA CGG CCA GTG	attacctg	CGTTTTTCGTGCGCCGCTTC	G5	27f_PL077	GTA AAA CGA CGG CCA GTG	gtcatacg	CGTTTTTCGTGCGCCGCTTC
C5	27f_PL029	GTA AAA CGA CGG CCA GTG	attctaat	CGTTTTTCGTGCGCCGCTTC	G6	27f_PL078	GTA AAA CGA CGG CCA GTG	gtgcatat	CGTTTTTCGTGCGCCGCTTC
C6	27f_PL030	GTA AAA CGA CGG CCA GTG	cacaagga	CGTTTTTCGTGCGCCGCTTC	G7	27f_PL079	GTA AAA CGA CGG CCA GTG	gttgtaga	CGTTTTTCGTGCGCCGCTTC
C7	27f_PL031	GTA AAA CGA CGG CCA GTG	cacaccct	CGTTTTTCGTGCGCCGCTTC	G8	27f_PL080	GTA AAA CGA CGG CCA GTG	gtttggtt	CGTTTTTCGTGCGCCGCTTC
C8	27f_PL032	GTA AAA CGA CGG CCA GTG	cagagagt	CGTTTTTCGTGCGCCGCTTC	G9	27f_PL081	GTA AAA CGA CGG CCA GTG	taaatcag	CGTTTTTCGTGCGCCGCTTC
C9	27f_PL033	GTA AAA CGA CGG CCA GTG	cagtaatg	CGTTTTTCGTGCGCCGCTTC	G10	27f_PL082	GTA AAA CGA CGG CCA GTG	taaggacg	CGTTTTTCGTGCGCCGCTTC
C10	27f_PL034	GTA AAA CGA CGG CCA GTG	catctggg	CGTTTTTCGTGCGCCGCTTC	G11	27f_PL083	GTA AAA CGA CGG CCA GTG	taatgtat	CGTTTTTCGTGCGCCGCTTC
C11	27f_PL035	GTA AAA CGA CGG CCA GTG	catgggtc	CGTTTTTCGTGCGCCGCTTC	G12	27f_PL084	GTA AAA CGA CGG CCA GTG	taggcgac	CGTTTTTCGTGCGCCGCTTC
C12	27f_PL036	GTA AAA CGA CGG CCA GTG	catttctt	CGTTTTTCGTGCGCCGCTTC	H1	27f_PL085	GTA AAA CGA CGG CCA GTG	tataatgc	CGTTTTTCGTGCGCCGCTTC
D1	27f_PL037	GTA AAA CGA CGG CCA GTG	ccagacct	CGTTTTTCGTGCGCCGCTTC	H2	27f_PL086	GTA AAA CGA CGG CCA GTG	tccaccga	CGTTTTTCGTGCGCCGCTTC
D2	27f_PL038	GTA AAA CGA CGG CCA GTG	ccccgctt	CGTTTTTCGTGCGCCGCTTC	H3	27f_PL087	GTA AAA CGA CGG CCA GTG	tccctgct	CGTTTTTCGTGCGCCGCTTC
D3	27f_PL039	GTA AAA CGA CGG CCA GTG	ccctatgt	CGTTTTTCGTGCGCCGCTTC	H4	27f_PL088	GTA AAA CGA CGG CCA GTG	tccttata	CGTTTTTCGTGCGCCGCTTC
D4	27f_PL040	GTA AAA CGA CGG CCA GTG	ccgaaaac	CGTTTTTCGTGCGCCGCTTC	H5	27f_PL089	GTA AAA CGA CGG CCA GTG	tcgagtcc	CGTTTTTCGTGCGCCGCTTC
D5	27f_PL041	GTA AAA CGA CGG CCA GTG	ccgattgg	CGTTTTTCGTGCGCCGCTTC	H6	27f_PL090	GTA AAA CGA CGG CCA GTG	tcggcttg	CGTTTTTCGTGCGCCGCTTC
D6	27f_PL042	GTA AAA CGA CGG CCA GTG	ccgcgtaa	CGTTTTTCGTGCGCCGCTTC	H7	27f_PL091	GTA AAA CGA CGG CCA GTG	tcggtcat	CGTTTTTCGTGCGCCGCTTC
D7	27f_PL043	GTA AAA CGA CGG CCA GTG	ccggcggt	CGTTTTTCGTGCGCCGCTTC	H8	27f_PL092	GTA AAA CGA CGG CCA GTG	tctgaaag	CGTTTTTCGTGCGCCGCTTC
D8	27f_PL044	GTA AAA CGA CGG CCA GTG	cctccccc	CGTTTTTCGTGCGCCGCTTC	H9	27f_PL093	GTA AAA CGA CGG CCA GTG	tgattcca	CGTTTTTCGTGCGCCGCTTC
D9	27f_PL045	GTA AAA CGA CGG CCA GTG	cgaaacta	CGTTTTTCGTGCGCCGCTTC	H10	27f_PL094	GTA AAA CGA CGG CCA GTG	tgcatctt	CGTTTTTCGTGCGCCGCTTC
D10	27f_PL046	GTA AAA CGA CGG CCA GTG	cgactgtt	CGTTTTTCGTGCGCCGCTTC	H11	27f_PL095	GTA AAA CGA CGG CCA GTG	tgcccaat	CGTTTTTCGTGCGCCGCTTC
D11	27f_PL047	GTA AAA CGA CGG CCA GTG	cgcaggcg	CGTTTTTCGTGCGCCGCTTC	H12	27f_PL096	GTA AAA CGA CGG CCA GTG	tggcttgc	CGTTTTTCGTGCGCCGCTTC
D12	27f_PL048	GTA AAA CGA CGG CCA GTG	cggcccgg	CGTTTTTCGTGCGCCGCTTC					
E1	27f_PL049	GTA AAA CGA CGG CCA GTG	cggtctcc	CGTTTTTCGTGCGCCGCTTC					

2.9 – Preparing TEM Grids

Microscopy was performed on phage lysates that were considered purified and high titer. 10 μL of filtered lysate was incubated for 3–10 minutes on Carbon Type–B, 300 mesh copper grids. Grids were washed twice with mqH_2O and stained with filtered 1% uranyl acetate. Grids were imaged at 80–120kV, and images were assembled using FIJI.

Note: In some cases where imaging was performed but a poor image was achieved, either with dismembered virions, poor image quality, or background noise, several optimizations were tested. In particular, the use of nuclease treatment and PEG precipitation on phage lysates was effective in reducing background noise. Additionally, supplementing lysates with Tween 20 was effective in reducing adhesion of phage particles during the washing process.

2.10 – Phage Genome Extraction

PEG Precipitation

>10 mL of high titer lysate (>$1x10^9$ pfu/mL) was filtered through a 0.22 μm filter and treated with DNaseI (5 mg/mL) to 0.03% and unboiled RNase A (10 mg/mL) to 0.15% and incubated overnight at 37ºC. PEG precipitation buffer was added to a 1:4 ratio, mixed by inversion, and incubated at 4ºC for 4–5 hours. Lysates with PEG were centrifuged at 15,000 x g for 30 minutes at 4ºC, supernatant was removed, and tubes were re–spun at 5000 x g for 2 minutes. Supernatant was removed and pellets were resuspended in 500 μL – 1 mL of 15 mM EDTA. Solution was treated with 4 μL/mL Proteinase K and 50 μl/mL of 10% SDS and incubated at 55ºC for 30 minutes.

Phenol–Chloroform Extraction and EtOH Precipitation

Phenol/chloroform was added in a 1:1 ratio with nuclease treated lysate into a phase lock tube. Tubes were vortexed for 1 minute and then spun at 14,800 rpm for 5 minutes. Aqueous layer was transferred into a new phase lock tube and previous step was repeated. Aqueous layer was treated

with 500 µL of chloroform, vortexed 30 seconds, and spun at 14,800 rpm for 2 minutes. This step was repeated until a clear interface was visible between the aqueous and organic layers. The aqueous layer was transferred into separate tube, and 1/10th volume of 3M NaOAc, pH 5.2 was added in addition to 2.5 volumes of 100% ethanol. Tubes were mixed by end–over–end inversion and incubated at –20ºC for 1 hour or at 4ºC overnight, until a precipitate was visible. Samples were spun at 14,800 rpm for 5 minutes, until a pellet was visible, and ethanol was removed. Pellets were washed with 1 mL of 70% ethanol, gently vortexed, and briefly spun. Ethanol was removed and tubes were placed open for 10–20 minutes to allow residual ethanol to evaporate. Once pellet was dry, 50–100 µL TE was added, vortexed and spun briefly, and incubated at 4ºC overnight. If the pellet had not completely dissolved, sample was heated at 55ºC–65ºC for 30–60 minutes, then all DNA was pooled. DNA concentration and purity was confirmed by running 1–5 µL on a 1% agarose gel in 1X TAE at 110V for 30–60 minutes alongside a 1 kB or 100 bp DNA ladder.

2.11 – Restriction Digests

Phage DNA was heated at 65ºC for 10–15 minutes. 0.25–1 µg phage DNA was mixed with 2 µL of 10X restriction enzyme buffer, 0.2 µL RNAse A, 0.5 µL restriction enzyme, and mqH_2O up to 20 µL. Samples were incubated at 37ºC for 30–60 minutes. 4 µL of DNA loading dye was added to digested DNA, and 24 µL was run on a 1% agarose gel in 1X TAE at 110V for 30–90 minutes alongside a 1 kB or 100 bp DNA ladder.

2.12 – Host Range

Phages of interest were prepared at 1x10^8 pfu/mL and were serially diluted from 10^{-1} – 10^{-6} in a 96–well microtiter dish. Lawns of *Staphylococcal* strains of interest were prepared in duplicate on TGY plates. 5 µL of each phage dilution was spotted onto lawns, and plates were incubated at 34ºC overnight and imaged. In heat maps, red indicates high infection similar to activity on

isolation host, orange indicates moderate infection, yellow indicates low infection, cream indicates possible infection or infection from without, while indicates no infection, grey indicates not tested.

2.13 – Growth Curves

Overnight cultures of *S. epidermidis* were grown from single colonies in 25 mL of TGY as described in Chapter 2.1. Cultures were diluted to an optical density (OD) 600 0.1, then grow to exponential phase (OD600 ~0.4 – 0.8), and diluted back to OD600 0.1 once more to begin the growth curve. 200 µL of sample was inoculated into each well of a 24–well polystyrene plate. 20 µL of phage at varying MOI was added to wells in 3–4 replicates. TGY and MOI 0 negative controls were used. Plate was entered into microplate reader with the lid on under continuous orbital shaking at 34ºC for 16–24 hours where OD600 was measured every 15 minutes.

2.14 – Lysogens

50 µL of host bacteria was diluted from 10^{-1} – 10^{-6}. 5 TGY plates were seeded with 200 µL of $5x10^{8}$ pfu/mL phage using glass beads, and plates were set at room temperature to dry. 100 µL of each dilution of host bacteria was plated on the 5 phage seeded plates, and 5 control plates with no phage. Plates were incubated at 34ºC for 24–36 hours. Efficiency of Lysogeny (EOL) was calculated from a plate containing 50-200 colonies using the following equation: $EOL = \left[\frac{(CFU\ on\ phage\ seeded\ plate)}{(CFU\ on\ control\ plate)}\right] x100$. 4 well-isolated single colonies were picked from a dilution of the phage and control plates and suspended in 50 µL of PB. 5 µL was spotted onto a TGY plate and another 5 µL onto a TGY plate with TA and host lawn. Spots were dried at room temperature then struck for single colonies. Plates were incubated at 34ºC for 24–36 hours, and single colonies that released phage showed clearing on the plate with host. In cases where this occurred, 2 colonies were selected and streaking process was repeated to confirm phage release. If confirmed, a single

colony was inoculated into 20 mL TGY and grown at 220 rpm at 34ºC for 24–36 hours. 750uL of this lysogen culture was mixed with 250 μL of 80% glycerol and archived at -80ºC.

2.15 – Biofilms in 24–Well Polystyrene Plates

Biofilm Growth

Overnight cultures of *S. epidermidis* were grown from single colonies in 25 mL of TSB as described in Chapter 2.1. Cultures were diluted to OD600 of 0.1 and 1 mL was added to assay wells of sterile 24–well polystyrene plate in 3–4 replicates. Plates were covered with a lid and transferred to 34ºC for 24 hours under static conditions. OD600 was measured to quantify overall growth (biofilm and planktonic) in each well. Liquid culture containing planktonic cells was removed from each well by inverting plate and slight flicking motion to discard liquid. Each well was then washed with mqH2O by pipetting 1 mL of water directly against the side of the wells slowly while tilting the plate, wash solution was decanted as above. Biofilm cells were fixed prior to staining by incubation of washed plate face up with lid removed at 60ºC for 45–60 minutes. Wells were then stained with 200 μL 0.1% crystal violet stain (CV) by pipetting against the wall of each well and incubated at room temperature for 5 minutes. Excess stain was removed by washing in the same method as described above with mqH2O, repeated 3–4 times. Plates were left inverted to dry overnight, and wells were imaged with a handheld camera the following day.

Biofilm formation of NRRL 41021 was analyzed under various growth conditions for optimization: TSB media vs. TGY media; TSB media vs. TSB + 1% glucose, TSB + 2mM $CaCl_2$, or TSB + 2mM $MgCl_2$; and TSB media vs. TSB media + 1% glucose, 2mM $CaCl_2$, and 2mM $MgCl_2$. TSB media was observed to be far more effective than TGY media in promoting biofilm formation by NRRL 41021, where biofilms were able to attach better to the plate and appeared thicker. No visible difference was observed with the different TSB supplementations compared

with TSB alone. TSB media contains glucose and other minerals; thus, the additional supplementation was likely not necessary. As a result of these optimizations, subsequent biofilms were all grown in TSB media.

Biofilm Inhibition with Phage

Biofilm inhibition assays were performed following the protocol described above, where phage diluted in phage buffer was added in varying MOI at the same time as addition of diluted cultures to 24–well plate. Plates were incubated, washed, fixed, stained, and imaged as described above. MOI 0 served as negative control.

Biofilm Destruction with Phage

Biofilm destruction assays were performed following the "Biofilm Growth" protocol described above, where phage was added in varying MOI following the first wash step and prior to fixing. Phage diluted in phage buffer was added by pipetting against the wall of each well, and incubated under static conditions at 34ºC for 6–24 hours. Plates were incubated, washed, fixed, stained, and imaged as described above. MOI 0 served as negative control.

2.16 – Recipes

0.1% Crystal Violet Dye

2 g of crystal violet powder was added into 20 mL of 100% ethanol and dissolved overnight. 80 mL of mqH_2O was added and mixed until fully dissolved. Solution was filtered through 0.45 μm filter and stored in a dark glass bottle. Dye must be filtered before each use after 3 weeks.

TGY Liquid Media

5 g tryptone, 5 g yeast extract, 1 g K_2HPO_4, and 1 g dextrose were mixed in 1 L mqH_2O and autoclaved. Once cooled to ~55ºC, 1 mL 1M $CaCl_2$ and 1 mL 1000X cycloheximide was added.

TSB Liquid Media

30 g TSB powder was mixed in 1 L mqH_2O and autoclaved. Once cooled to ~55ºC, 1 mL 1000X cycloheximide was added.

TGY Top Agar

5 g tryptone, 5 g yeast extract, and 3 g agar were mixed in 1 L mqH_2O and autoclaved. Once cooled to ~55ºC, 2.5 mL 40% dextrose, 1 mL 1mM $CaCl_2$, and 1 mL 1M $MgSO_4$ was added.

TGY top agar recipe was adjusted based on potential peroxide formation due to reactions between K_2HPO_4 and agar when autoclaving, which may have interfered with successful phage infection on plates (47). Moreover, agar concentration was reduced from 0.4% to 0.3% to promote phage diffusion and adsorption, to promote clearer and larger plaquing (48).

TSB Top Agar

30 g TSB powder and 4 g agar were mixed in 1 L mqH_2O and autoclaved. Once cooled to ~55ºC, 1 mL 1 mM $CaCl_2$ was added.

TGY Plates

5 g tryptone, 5 g yeast extract, 1 g K_2HPO_4, 1 g dextrose, and 15 g agar were mixed into 1 L mqH_2O and autoclaved. Once cooled to ~55ºC, 1 mL 1M $CaCl_2$ and 1 mL 1000X cycloheximide was added and poured into petri dishes.

TSB Plates

30 g TSB powder and 15 g agar were mixed into 1 L mqH_2O and autoclaved. Once cooled to ~55ºC, 1 mL 1M $CaCl_2$ and 1 mL 1000X cycloheximide was added and poured into petri dishes.

PEG Precipitation Buffer

30 g Polyethylene glycol (PEG) 8000 and 19.3 g NaCl was dissolved in 100 mL mqH_2O over several hours at 4ºC. Once dissolved, buffer was filter–sterilized and stored at room temperature.

Phage Buffer

10 mL 1M tris (pH 7.5), 10 mL 1M $MgSO_4$, 4g NaCl, 10 mL 100mM $CaCl_2$, 100 mL 100% glycerol were dissolved into 1 L mqH_2O. Once dissolved, buffer was filter–sterilized and stored at room temperature.

Chapter 3 – Results

3.1 – Creation of a Diverse Collection of *S. epidermidis* Phages

3.1.1– Establishing S. epidermidis strains used in the collection

A diverse set of 13 *Staphylococcus epidermidis* and 1 *Staphylococcus succinus* strains from the USDA-ARS Culture Collection (NRRL) and American Type Culture Collection (ATCC) were cultured for use in this project (Table 1) (49, 50). These strains were primarily selected based on Bio-Safety Level 1 (BSL–1) distinction and diverse isolation source, where these strains were originally isolated from food, beverage, animals, and human infection. This broad strain selection was intended to examine if isolation host impacts the diversity of phages found, as is seen in Actinobacteriophages, and to generate a broad collection of phages to compare host range (see Chapter 3.3.1) (51).

All strains sourced from NRRL are not sequenced; thus, little is known about them, apart from their isolation source. However, the ATCC 35984 strain is sequenced and is quite relevant in the literature; known to be a strong biofilm former with production of adhesin proteins, methicillin-resistant, and encoding a CRISPR-Cas Defence system (52, 53). The ATCC 700337 strain is also genome sequenced and is a type strain of *S. succinus* (54).The *S. succinus* strain was included within this *S. epidermidis*-focused project to test potential cross-species infection by phages in the collection. Overlapping host range has been observed between these species, and *S. epidermidis* phages are reported to be more easily amplified on *S. succinus* (2).

3.1.2 – S. epidermidis bacteriophages can be isolated directly from skin

S. epidermidis bacteriophages were isolated from skin swab samples from healthy human volunteers, a workflow adapted from the SEA-PHAGES program and the protocol described in a study by Valente and colleagues (42, 43). Since May 2024, nearly 100 bacteriophages have been

isolated against *Staphylococcus epidermidis* and *Staphylococcus succinus* through this pipeline. 160 individuals consisting of University of Ottawa students, faculty members, members of the scientific community, and volunteers from the Ottawa area have donated a total of 265 samples. In most cases, if a particular volunteer's sample yielded multiple phages on the same/different hosts, only a single phage was pursued. Additionally, several hosts yielded phages that were difficult to amplify and therefore were not pursued further.

Several sampling events were organized throughout the duration of this project, with success rates reflecting improvements in the workflow. An organized sampling event at uOttawa Phage Camp in July 2024 consisted of 13 volunteers from the Ottawa area who donated a total of 35 samples, all of which were tested on 12 *S. epidermidis* hosts (excluding ATCC 35984 and ATCC 700337). 10 samples from 3 volunteers from this event yielded phage, with only 5 of these phages successfully amplifiable for archiving and further investigation, an isolation success rate of 29%. Another larger organized sampling event in June 2025 included 66 scientific volunteers consisting of Canadian Society of Microbiology conference attendees, TinyEarth Scientific Training attendees, and University of Ottawa researchers, who each donated a single sample. These volunteers were from areas across Canada; including Ontario, Quebec, Alberta, and British Columbia, and the USA; including California, North Dakota, New York, and Philadelphia, in addition to one volunteer from Beijing, China. Samples were tested on *S. epidermidis* NRRL 41021, NRRL 41129, NRRL 41142, and *S. succinus* ATCC 700337. A total of 37 samples successfully yielded phage on one or more isolation hosts, a success rate of 56%. 20 phages were purified, amplified, sequenced, and included in the collection. Between these two events, modifications were made to the sampling instructions to improve the likelihood of finding phage on a particular sample. These modified instructions emphasized factors surrounding cleanliness

and bodily location of samples, included recommendations to engage in physical activity to promote bacterial growth, sampling prior to showering, and using one swab across multiple body parts. Additionally, several strains were removed from the isolation process due to repeated poor success in finding phages on these hosts, including NRRL 41251, NRRL 41253, NRRL 41575, NRRL 41577, NRRL 4268, and NRRL 2616. We think the ~30% increase in success rate between the two sampling events is reflective of these changes and which have additionally cut costs and sped up the isolation process. Optimized isolation and characterization protocols were successfully implemented in the TMM3009 Bacteriophage Discovery Laboratory in 2024 and 2025, where 32 students contributed phages to our growing collection.

A total of 79 phages were reported in this collection, where 64 phages were archived for future use. Of this collection, sequencing information was recorded for 77 phages (Table 2). 71 phages were isolated against 7 laboratory strains of *Staphylococcus epidermidis*; NRRL 41021 [28], NRRL 41571 [13], NRRL 41129 [14], NRRL 41142 [5], ATCC 35984 [8], NRRL 41570 [1], NRRL 41574 [1] and 1 strain of *Staphylococcus succinus*; ATCC 700337 [8]. As stated previously, no phages were found to infect *S. epidermidis* NRRL 41251, NRRL 41253, NRRL 41575, NRRL 41577, NRRL 4268, and NRRL 2616.

Table 2. Characterization of *S. epidermidis* Bacteriophage Collection. 79 bacteriophages have been isolated for this collection. Hosts are grouped by colour. 'Y' indicates phages that were archived, 'N' indicates phages that were not archived, but were sequenced. Structural morphotype is determined by transmission electron microscopy.

#	Phage	Host	Archived?	Morphotype
1	**Untouchable**	*S. epidermidis* 41021	Y	N/A
2	**Morvex**	*S. epidermidis* 41021	Y	Myovirus
3	**Teegee**	*S. epidermidis* 41021	Y	Myovirus
4	**Snowbeep**	*S. epidermidis* 41021	Y	Siphovirus
5	**Flume**	*S. epidermidis* 41021	Y	Myovirus
6	**Pheter**	*S. epidermidis* 41021	Y	Myovirus
7	**FoolishOne**	*S. epidermidis* 41021	Y	Myovirus
8	**Kozzy**	*S. epidermidis* 41021	Y	Myovirus
9	**SillyBilly**	*S. epidermidis* 41021	Y	Myovirus
10	**Gord**	*S. epidermidis* 41021	Y	Myovirus
11	**Tfoot715**	*S. epidermidis* 41571	Y	Siphovirus
12	**Goopey**	*S. epidermidis* 41021	Y	Siphovirus
13	**Mewtwo72**	*S. epidermidis* 41021	Y	Myovirus
14	**Squishfish**	*S. epidermidis* 41571	Y	Siphovirus
15	**Megalynn**	*S. epidermidis* 41021	Y	Siphovirus
16	**LilKati**	*S. epidermidis* 41021	Y	Myovirus
17	**LoPharo**	*S. epidermidis* 41021	Y	Myovirus
18	**Concordia**	*S. epidermidis* 41571	Y	Siphovirus
19	**Gamble**	*S. epidermidis* 41571	Y	Siphovirus
20	**Nosalina**	*S. epidermidis* 41571	Y	Siphovirus
21	**Novi248**	*S. epidermidis* 41571	Y	Siphovirus
22	**Boojo**	*S. epidermidis* 41021	Y	Siphovirus
23	**Maqloubeh**	*S. epidermidis* 41021	Y	Siphovirus
24	**Trammy**	*S. epidermidis* 41021	Y	Siphovirus
25	**Luntik**	*S. epidermidis* 41571	Y	Siphovirus
26	**Khosrow**	*S. epidermidis* 41571	Y	Siphovirus
27	**Puddums**	*S. epidermidis* 41571	Y	Siphovirus
28	**Beerus**	*S. epidermidis* 41571	Y	Siphovirus
29	**Valverde8**	*S. epidermidis* 41021	Y	Siphovirus
30	**Harppy**	*S. epidermidis* 41021	Y	Myovirus
31	**SamJr**	*S. epidermidis* 41129	Y	Siphovirus
32	**Basmrit**	*S. epidermidis* 41129	Y	Myovirus
33	**Emma**	*S. epidermidis* 41021	N	N/A
34	**Nuvai**	*S. epidermidis* 41570	Y	Siphovirus
35	**Farolita**	*S. epidermidis* 41142	Y	Siphovirus
36	**Zomp**	*S. epidermidis* 35984	Y	N/A
37	**Succo**	*S. succinus* 700337	N	N/A
38	**Adam**	*S. succinus* 700337	Y	N/A
39	**Alex**	*S. succinus* 700337	Y	Myovirus
40	**Franklin**	*S. succinus* 700337	Y	Myovirus
41	**Brandon**	*S. epidermidis* 41571	Y	Siphovirus
42	**BJ**	*S. epidermidis* 41571	Y	N/A
43	**Egert**	*S. epidermidis* 41571	Y	N/A

44	**#159**	*S. epidermidis* 41142	N	N/A
45	**#168**	*S. epidermidis* 41021	N	N/A
46	**#170**	*S. epidermidis* 41021	N	N/A
47	**Evora**	*S. epidermidis* 41142	N	N/A
48	**#172**	*S. epidermidis* 41129	N	N/A
49	**Infinity**	*S. succinus* 700337	N	N/A
50	**Udeam**	*S. succinus* 700337	Y	N/A
51	**#179**	*S. succinus* 700337	N	N/A
52	**Rubyro**	*S. succinus* 700337	Y	N/A
53	**#184**	*S. epidermidis* 41021	N	N/A
54	**#187**	*S. epidermidis* 41129	N	N/A
55	**Remoras**	*S. epidermidis* 41129	Y	N/A
56	**Dueto**	*S. epidermidis* 41129	N	N/A
57	**#192**	*S. epidermidis* 41021	N	N/A
58	**#193**	*S. epidermidis* 41021	N	N/A
59	**Pilgrim**	*S. epidermidis* 41129	N	N/A
60	**Kipko**	*S. epidermidis* 41129	Y	N/A
61	**#214**	*S. epidermidis* 41021	N	N/A
62	**Amber**	*S. epidermidis* 41129	Y	N/A
63	**Mocanita**	*S. epidermidis* 41021	Y	Myovirus
64	**Athee**	*S. epidermidis* 41574	Y	Myovirus
65	**Sachers**	*S. epidermidis* 35984	Y	Myovirus
66	**Hollyann**	*S. epidermidis* 41142	Y	Siphovirus
67	**Mooshii**	*S. epidermidis* 41142	Y	Siphovirus
68	**TerrificDeevas**	*S. epidermidis* 35984	Y	Myovirus
69	**Medieval**	*S. epidermidis* 41129	Y	Siphovirus
70	**Zoomy**	*S. epidermidis* 35984	Y	Myovirus
71	**Constellation**	*S. epidermidis* 41129	Y	Siphovirus
72	**Dazz**	*S. epidermidis* 35984	Y	Siphovirus
73	**Dicey**	*S. epidermidis* 35984	Y	Myovirus
74	**Fashfush**	*S. epidermidis* 35984	Y	Myovirus
75	**Wagyu**	*S. epidermidis* 41129	Y	Myovirus
76	**GojoSatoru**	*S. epidermidis* 35984	Y	Myovirus
77	**Bigbac**	*S. epidermidis* 41129	Y	Siphovirus
78	**Valiant**	*S. epidermidis* 41129	Y	Siphovirus
79	**Mosuto**	*S. epidermidis* 35984	Y	Myovirus

3.1.3 – S. epidermidis phages may be Myoviruses or Siphoviruses

Transmission electron microscopy (TEM) was used to visualize and identify phage morphotype. This work identified 25 Myoviruses and 28 Siphoviruses, where only the images for phages selected for the subset later described in Chapter 3.3 were shown (Figure 1). No Podoviruses were found in this collection.

Measurements of phage capsids and tails allows comparison between phages and morphotypes. Capsid size is often relative to genome size, and this is visible amongst our phages, as Cluster C Myoviruses have much larger capsids compared to Siphoviruses. Additionally comparing tail measurements may distinguish Myoviruses from Siphoviruses. This is visible in our phages, where the Siphoviruses have much longer tails than the Myoviruses, and additionally where their >300nm is consistent with what is described in the literature for Cluster D Siphoviruses. Goopey is an exception, where its tail length measured 194nm. This shorter tail length may be indicative that part of the tail was broken off prior to imaging or may represent uniqueness in its structural morphology.

Several Myoviruses were observed in their contracted and extended tail conformations, a feature of their contractile tail machinery (Figure 2). This phenomenon is attributed to a premature tail contraction and has been reported to occur in other Myoviruses. This change may be triggered by conditions that mimic or force a structural shift, including exposure to molecules resembling bacterial surface receptors, or exposure to unfavourable conditions (pH, temperature, osmotic pressure) which may cause premature tail contraction (55). 26 phages in this collection remain unclassified by TEM, as they were either not amplifiable to high enough titers, were poor quality images, or were not selected to be imaged.

A

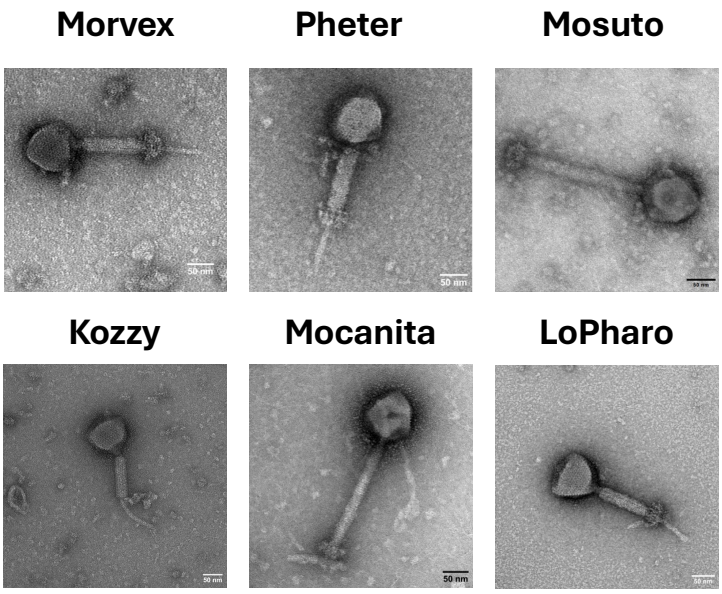

C

Phage	Capsid (nm)	Tail (nm)
Morvex	89x85	259
Pheter	88x76	215
Mosuto	100x90	247
Kozzy	100x96	268
Mocanita	96x92	239
LoPharo	101x95	221
Snowbeep	79x76	377
Trammy	63x63	396
BigBac	71x65	374
Goopey	73x69	194

B

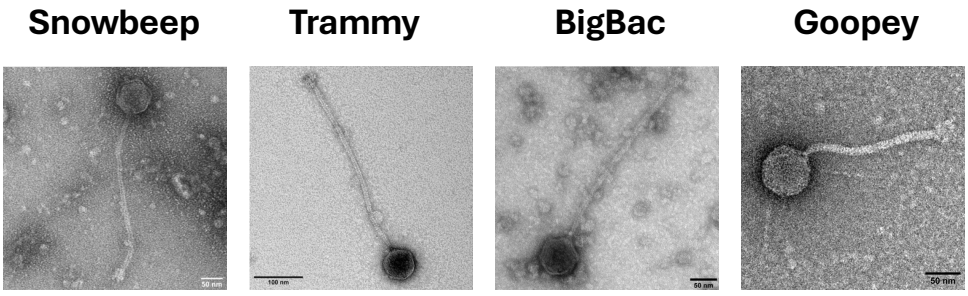

Figure 1. Diverse *Staphylococcus epidermidis* Bacteriophages Exist in Siphovirus and Myovirus Morphologies. Phage lysate was incubated on a carbon grid, stained with 1% uranyl acetate, and imaged at 80–120kV. **A. Cluster C Myoviruses.** Morvex, Pheter, Mosuto, Kozzy, Mocanita, and LoPharo. **B. Cluster D Siphoviruses.** Snowbeep, Trammy, BigBac, and Goopey. **C.** Capsid and tail measurements. *Myoviridae* tail lengths calculated from extended state.

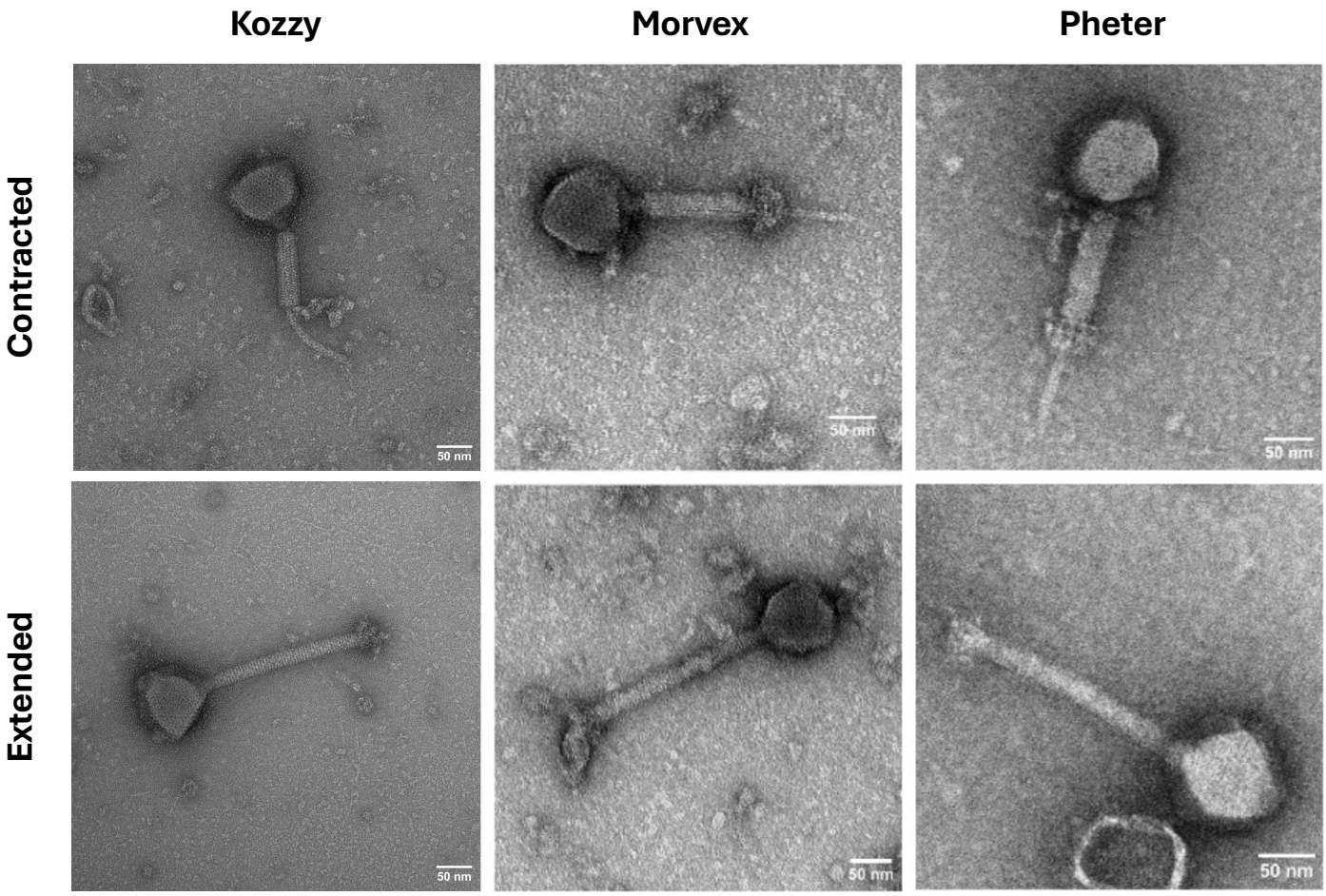

Figure 2. Extended and Contracted Tail States of *S. epidermidis* Myoviruses. Phage lysate was incubated on a carbon grid, stained with 1% uranyl acetate, and imaged at 80–120kV. Cluster C Myoviruses Kozzy, Morvex, and Pheter are shown in the contracted (top) and extended (bottom) states.

3.2 – Genomic Characterization of *Staphylococci* Bacteriophages

Genomic sequencing offers insight into phylogenetic relationships between phages and allows clustering into groups of similar phages; this information was used to determine which phages were pursued further. Isolated phages are sequenced by Oxford Nanopore long-read sequencing and/or the Illumina MiSeq Platform to elucidate genomic diversity, and results were analyzed by NCBI Nucleotide Blast to assess similarity to existing *S. epidermidis* bacteriophages (56). In conjunction with Kieran Furlong, Celina Tanbari, and the 2024 and 2025 TMM 3009 Phage Discovery classes, 77 of the 79 phages in this collection have been successfully sequenced, having obtained sufficient data to interpret clustering and phylogenetic relationships for most (Table 3).

3.2.1 – Genomic sequencing of Staphylococcal phages

Genomic sequencing and clustering provides preliminary data regarding phage uniqueness and relatedness within the collection, and offers insight into what phages may be suitable for phage therapy. At the beginning of this project, phages were sequenced at The University of Ottawa by Oxford Nanopore long-read sequencing of extracted phage DNA genomes. This methodology requires high-titer amplification and DNA extraction of each phage of interest, often taking weeks to obtain suitable DNA for sequencing of a single phage. In these early efforts, genomic DNA was fragmented by either sonication or MuA-dependent transposition (tagmentation) and barcoded using ligation or tagmentation. In both the ligation and transposition approaches, phage DNA is directly sequenced. These two approaches yielded only short reads that couldn't be assembled into a single contig.

Since summer 2025, newly isolated phages are sequenced at The University of Ottawa by a novel direct-from-plaque Oxford Nanopore long-read sequencing protocol developed by a research team at McGill University (Figure 3) (44). This methodology permits rapid sequencing

of up to 96 newly isolated phages per run, and eliminates time spent on phage amplification and DNA extraction, allowing us to focus only on phages of interest. Using this technique we have obtained 19 complete genomes, defining a complete genome as ones that produced a circular contig or where a linear contig was within 10% of the genome length of the closest match (Table 3) (56). An additional 58 phages in our collection are determined to be partially sequenced. Two phages, LoPharo and Khosrow, were fully sequenced through Illumina Sequencing at The University of Pittsburgh and are complete (Table 3).

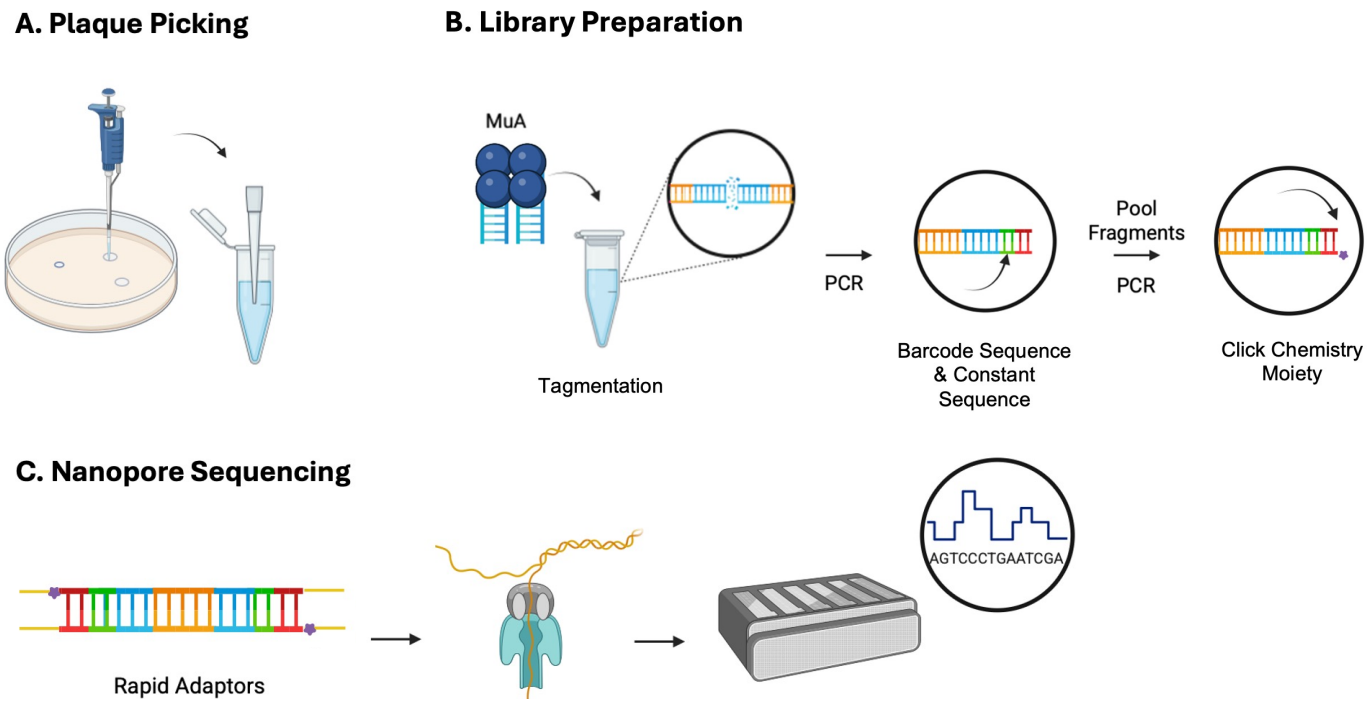

Figure 3. Flowchart of Nanopore Sequencing Protocol. A. Plaque Picking. Samples containing phage DNA are collected by sterile picking of a single plaque formed by a bacteriophage on a TGY agar plate with a lawn of *S. epidermidis*. The sample is suspended in TE buffer, briefly vortexed, and heated to release genomic material. **B. Library Preparation.** A MuA transposase is added, permitting transposase-mediated fragmentation (tagmentation) of phage DNA (orange) and addition of a MuA recognition sequence (blue). PCR is performed with a barcoded oligonucleotide containing a sequence that binds and amplifies the MuA sequence, a distinct barcode region (green), and a constant sequence (red). Barcoded fragments are pooled and balanced, and a second PCR is performed to amplify fragments using an oligonucleotide with a click chemistry moiety (purple). **C. Nanopore Sequencing.** Following amplification, rapid adaptors are added at the end of MuA fragments via click chemistry. Genomic DNA is sequenced on an ONT MinION R10.4.1 chemistry. Reads are assembled and analyzed by NCBI Nucleotide Blast to assess similarity to existing *S. epidermidis* bacteriophages. Created in BioRender. Protocol adapted from Brenna Fox and Patrick Lypaczewski from McGill University (44).

Table 3. Sequencing of *S. epidermidis* Bacteriophage Collection. Sequencing results were obtained through nanopore long-read sequencing (NP), unless indicated as Illumina sequencing (IL), and analyzed by pairwise genome alignment by NCBI Nucleotide Blast (56). Phage clustering is as determined by Olivieri et al. based on shared gene content (34). Complete sequences are within 10% of size of blast match and are highlighted in yellow.

Phage	Sequencing	Cluster	Match
Untouchable	35,344bp	C	*Staphylococcus* phage 80B (139,645bp): 99% QC, 99% ID
Morvex	41,751bp	C	*Staphylococcus* phage vB_SepM_BE04 (142,331bp); 100% QC, 99% ID
Teegee	22,660bp	C	*Staphylococcus* phage Terranova, (141,288bp) 100% QC, 98% ID
Snowbeep	83,980bp	D	*Staphylococcus* phage vB_SepS_BE22 (92,847bp); 90% QC, 97% ID
Flume	12,340bp	C	*Staphylococcus* phage 80B (139,645bp): 93% QC, 99% ID
Pheter	32,890bp	C	*Staphylococcus* phage vB_Sep_steph3 (140,342bp); 100% QC, 98% ID
FoolishOne	53,977bp	D	*Staphylococcus* phage S-CoN_Ph9 (89,830bp); 98% QC, 98% ID
Kozzy	28,837bp	C	*Staphylococcus* phage vB_Sep_steph3 (140,342bp); 100% QC, 98% ID
SillyBilly	28,747bp	C	*Staphylococcus* phage vB_Sep_steph3 (140,342bp); 100% QC, 98% ID
Gord	11,072bp	C	*Staphylococcus* phage vB_SepM_BE05 (140,271bp); 100% QC, 99% ID
Tfoot715	41,815bp	B	MAG: Caudoviricetes sp. Isolate MSP0103 genomic sequence (138,771bp); 58% QC, 94% ID
Goopey	27,003bp	D	*Staphylococcus* phage S-CoN_Ph9 (89,830bp); 98% QC, 99% ID
Mewtwo72	N/A		
Squishfish	40,397bp	B	MAG: Caudoviricetes sp. Isolate MSP0103 genomic sequence (138,771bp); 59% QC, 96% ID
Megalynn	42,113bp	B	MAG: Caudoviricetes sp. Isolate ctZgI1, partial gen. (45,878bp); 63% QC, 94% ID
LilKati	27,367bp	C	*Staphylococcus* phage 80B (139,645bp): 100% QC, 99% ID
LoPharo	142,448bp (IL)	C	*Staphylococcus* phage philPLA-C1C (140,961bp); 99% QC, 96% ID
Concordia	N/A		
Gamble	42,185bp	B	*Staphylococcus* phage PH15 (44,041bp); 71% QC, 94% ID
Nosalina	41,647bp	B	*Staphylococcus* phage vB_SepS_BE28 (42,841bp); 88% QC, 96% ID
Novi248	377bp	B	*Staphylococcus* phage vB_SepS_BE20 (43,521bp)

Boojo	41,438bp	B	MAG: Caudoviricetes sp. Isolate ctZgI1, partial gen. (45,878bp); 54% QC, 96% ID
Maqloubeh	14,564bp	B	MAG: Caudoviricetes sp. Isolate ctZgI1, partial gen. (45,878bp); 87% QC, 95% ID
Trammy	57,801bp	D	*Staphylococcus* phage vB_SepS_BE22 (92,847bp); 93% QC, 98% ID
Luntik	42,163bp	B	MAG: Caudoviricetes sp. Isolate MSP0206 genomic seq. (112,610bp); 64% QC, 95% ID
Khosrow	43,820bp (IL)	B	*Staphylococcus* phage PH15 (44,041bp); 65% QC, 93% ID
Puddums	39,410bp	B	MAG: Caudoviricetes sp. Isolate ctZgI1, partial gen. (45,878bp); 57% QC, 96% ID
Beerus	40,017bp	B	MAG: Caudoviricetes sp. Isolate ctZgI1, partial gen. (45,878bp); 56% QC, 96% ID
Valverde8	41,621bp	B	MAG: Caudoviricetes sp. Isolate ctZgI1, partial gen. (45,878bp); 54% QC, 97% ID
Harppy	43,215bp	C	*Staphylococcus* phage 80B (139,645bp); 100% QC, 97% ID
SamJr	44,985bp	B	MAG: Caudoviricetes sp. Isolate MSP0206 genomic seq. (112,610bp); 58% QC, 95% ID
Basmrit	30,766bp	C	*Staphylococcus* phage vB_SepM_BE25 (140,292 bp); 100% QC, 99% ID
Emma	42,113bp	B	MAG: Caudoviricetes sp. Isolate MSP0103 genomic sequence (138,771bp)
Nuvai	41,979bp	B	MAG: Caudoviricetes sp. Isolate MSP0206 genomic seq. (112,610bp); 66% QC, 95%ID
Farolita	43,668bp	B	*Staphylococcus* phage vB_SepS_E72 (44,592bp); 76% QC, 96% ID
Zomp	15,681bp	C	*Staphylococcus* phage 80B (139,645bp); 100% QC, 93% ID
Succo	22,944bp	C	*Staphylococcus* phage vB_Sep_steph3 (140,342bp); 100% QC, 98% ID
Adam	13,028bp	C	*Staphylococcus* phage 110 (141,747bp); 100% QC, 99% ID
Alex	29,324bp	C	*Staphylococcus* phage 80B (139,645bp); 100% QC, 99% ID
Franklin	31,241bp	C	*Staphylococcus* phage PG-2021_27 (128,279bp); 91% QC, 99% ID
Brandon	43,118bp	B	*Staphylococcus* phage vB_SepS_BE01 (42,718bp); 85% QC, 95% ID
BJ	41,869bp	B	*Staphylococcus* phage vB_SepS_BE01(42,718bp); 83% QC, 95% ID
Egert	23,280bp	B	MAG: Caudoviricetes sp. Isolate MSP0206 genomic seq. (112,610bp); 91% QC, 96% ID
#159	44,142bp	B	MAG: Caudoviricetes sp. Isolate MSP0206 genomic seq. (112,610bp); 58% QC, 96% ID
#168	42,295bp	B	MAG: Caudoviricetes sp. Isolate MSP0103 genomic seq. (138,771bp); 58% QC, 95% ID
#170	43,199bp	B	*Staphylococcus* phage vB_SepiS-philPLA7 (42,123bp); 72% QC, 91% ID

Evora	82,364bp	D	*Staphylococcus* phage 6ec (93,796bp); 87% QC, 94% ID
#172	43,018bp	B	*Staphylococcus* phage vB_SepiS-philPLA7 (42,123bp); 60% QC, 97% ID
Infinity	75,265bp	C	*Staphylococcus* phage PG-2021_27 (128,279bp); 90% QC, 97% ID
Udeam	38,589bp	C	MAG: Herelleviridae sp. Isolate ctdGG3, partial gen. (140,879bp); 100% QC, 93% ID
#179	44,444bp	B	*Staphylococcus* phage vB_SepS_E72 (44,592bp); 70% QC, 96% ID
Rubyro	30,821bp	C	*Staphylococcus* phage 80B(139,645bp); 96% QC, 99% ID
#184	25,838bp	C	*Staphylococcus* phage 80B (139,645bp); 95% QC, 99% ID
#187	23,616bp	D	*Staphylococcal* phage CF1 (96,354bp); 95% QC, 96% ID
Remoras	12,305bp	C	*Staphylococcus* phage Twillingate (142,592bp); 96% QC, 97% ID
Dueto	78,082bp	C	*Staphylococcus* phage Terranova (141,288bp); 93% QC, 96% ID
#192	13,804bp	C	*Staphylococcus* phage vB_SepM_philPLA-C1C (140,961bp); 98% QC, 99% ID
#193	14,100bp	B	MAG: Caudoviricetes sp. Isolate MSP0103 genomic sequence (138,771bp); 36% QC, 93% ID
Pilgrim	72,224bp	C	*Staphylococcus* phage Terranova (141,288bp); 96% QC, 98% ID
Kipko	30,725bp	C	*Staphylococcus* phage Terranova (141,288bp); 92% QC, 98% ID
#214	48,127bp	C	*Staphylococcus* phage philPLA-C1C (140,961bp); 94% QC, 97% ID
Amber	26,166bp	C	*Staphylococcus* phage Terranova (141,288bp); 92% QC, 95% ID
Mocanita	95,665bp	C	MAG: Herelleviridae sp. Isolate ctdGG3, partial gen. (140,879bp); 98% QC, 95% ID; Staphylococcus phage Terranova (141,288bp); 38% QC, 77% ID
Athee	26,016bp	C	*Staphylococcus* phage vB_Sep_steph3 (140,342bp); 100% QC, 97% ID
Sachers	29,870bp	C	*Staphylococcus* phage philPLA-C1C (140,961bp); 100% QC, 98% ID
Hollyann	44,137bp	B	*Staphylococcus* phage vB_SepS_E72 (44,592bp); 77% QC, 96% ID
Mooshii	42,949bp	B	MAG: Caudoviricetes sp. Isolate MSP0206 genomic seq. (112,610bp); 53% QC, 93% ID
TerrificDeevas	9,952bp	C	*Staphylococcus* phage 80B (139,645bp); 98% QC, 99% ID
Medieval	35,781bp	B	MAG: Caudoviricetes sp. Isolate MSP0206 genomic seq. (112,610bp); 66% QC, 95% ID
Zoomy	22,358bp	C	*Staphylococcus* phage 80B (139,645bp); 97% QC, 99% ID

Constellation	27,370bp	B	MAG: *Staphylococcus* phage HS13 (46,260bp); 100% QC, 97% ID
Dazz	8,029bp	C	*Staphylococcus* phage 80B (139,645bp); 99% QC, 99% ID
Dicey	8,020bp	C	*Staphylococcus* phage 110, complete gen. (141,747bp); 99% QC, 99% ID
Fashfush	7,554bp	C	*Staphylococcus* phage vB_SepS_BE06 (140,659bp); 100% QC, 98% ID
Wagyu	11,469bp	C	*Staphylococcus* phage vB_SepM_BE05 (140,271bp); 100% QC, 97% ID
GojoSatoru	25,558bp	C	*Staphylococcus* phage Terranova, (141,288bp) 94% QC, 98% ID
Bigbac	66,617bp	D	*Staphylococcal* phage CF1 (96,354bp); 96% QC, 99% ID
Valiant	42,941bp	B	*Staphylococcus* phage vB_SepiS-philPLA7, complete gen. (42,123bp); 68% QC, 97% ID
Mosuto	33,288bp	C	*Staphylococcus* phage vB_SepM_BE25 (140,292 bp); 98% QC, 97% ID

3.2.2 –Staphylococcal phages can be clustered and are genomically diverse

Phage sequences are organized into four distinct clusters based on shared gene content, as described in the 2019 study by Oliveira and colleagues (34). Sequenced phages in this collection cluster in 3 of these 4 distinct groups; 31 phages align to Cluster B, 39 phages align to Cluster C, and 7 phages align to Cluster D (Table 3). We have not determined any phages in this collection to be Cluster A. Only one Cluster C phage has been fully sequenced by Illumina Sequencing: LoPharo has a 142,448 bp genome that aligns to Cluster C *Staphylococcus* phage philPLA-C1C with 99% query cover and 94% sequence identity. Full genome sequences were obtained through Nanopore sequencing for Snowbeep (83,980 bp) and Evora (82,364 bp) aligning to Cluster D *Staphylococcus* phages vB_SepS_BE22, with 90% query cover and 97% sequence identity, and 6ec, with 87% query cover and 94% sequence identity, respectively. Full sequences were obtained for 16 Cluster B phages, including Megalynn (42,113 bp) and Khosrow (43,820 bp), which aligned to Cluster B phages ctZgI1 (45,878 bp) with 63% query cover and 94% sequence identity, and *Staphylococcus* phage PH15 (44,041 bp) with 65% query cover and 93% sequence identity, respectively. Of interest, Cluster C phage Mocanita (incomplete sequence: 95,665 bp) aligned to *Staphylococcus* phage ctdGG3 (partial sequence: 140,879 bp), with 98% query cover and 95% sequence identity, and Terranova (141,288 bp), with 38% query cover and 77% sequence identity, respectively. While sharing high similarity with the partial sequence of *Staphylococcus* phage ctdGG3, the low similarity of Mocanita to all other phage matches, indicates it is more unique and worth pursuing further. Phages with sequence similarity to Clusters A, C, and D may have potential for phage therapy use and were further characterized in Chapter 3.3, while temperate Cluster B phages were avoided.

Sequencing data is visualized by organization of genome sequences into a phylogenetic tree based on shared nucleotide similarity (Figure 4). Phylogenetic analysis reveals genetic diversity within the phage collection, with several phages exhibiting distinct evolutionary relationships. Notably, Cluster C phages Mocanita, Untouchable, Dueto, and Infinity, and Cluster D phages Bigbac and Goopey appear more genomically unique, diverging from an earlier common node, suggesting a lower degree of similarity to matches compared to other phages in their clusters. Additionally, Cluster C phages Zomp, Gord, and Flume diverge from a common node shared with a Cluster A Podoviruses including JBug18, Andhra, and St134, posing that these phages may be unique and distinct from other Cluster C phages in the group. Additionally, geographic distribution of the volunteer samples, described in Chapter 3.1.2, appeared to have no influence on the phages isolated, i.e. Phage179 isolated off a volunteer from Beijing, China, appeared phylogenetically similar to phage Mooshii, isolated off a volunteer from Ottawa, Canada. However, as many genome sequences included within this tree are incomplete (with complete sequences as indicated yellow highlight in Table 3), these results may not be fully accurate, and complete sequences must be attained to draw confident conclusions from this figure.

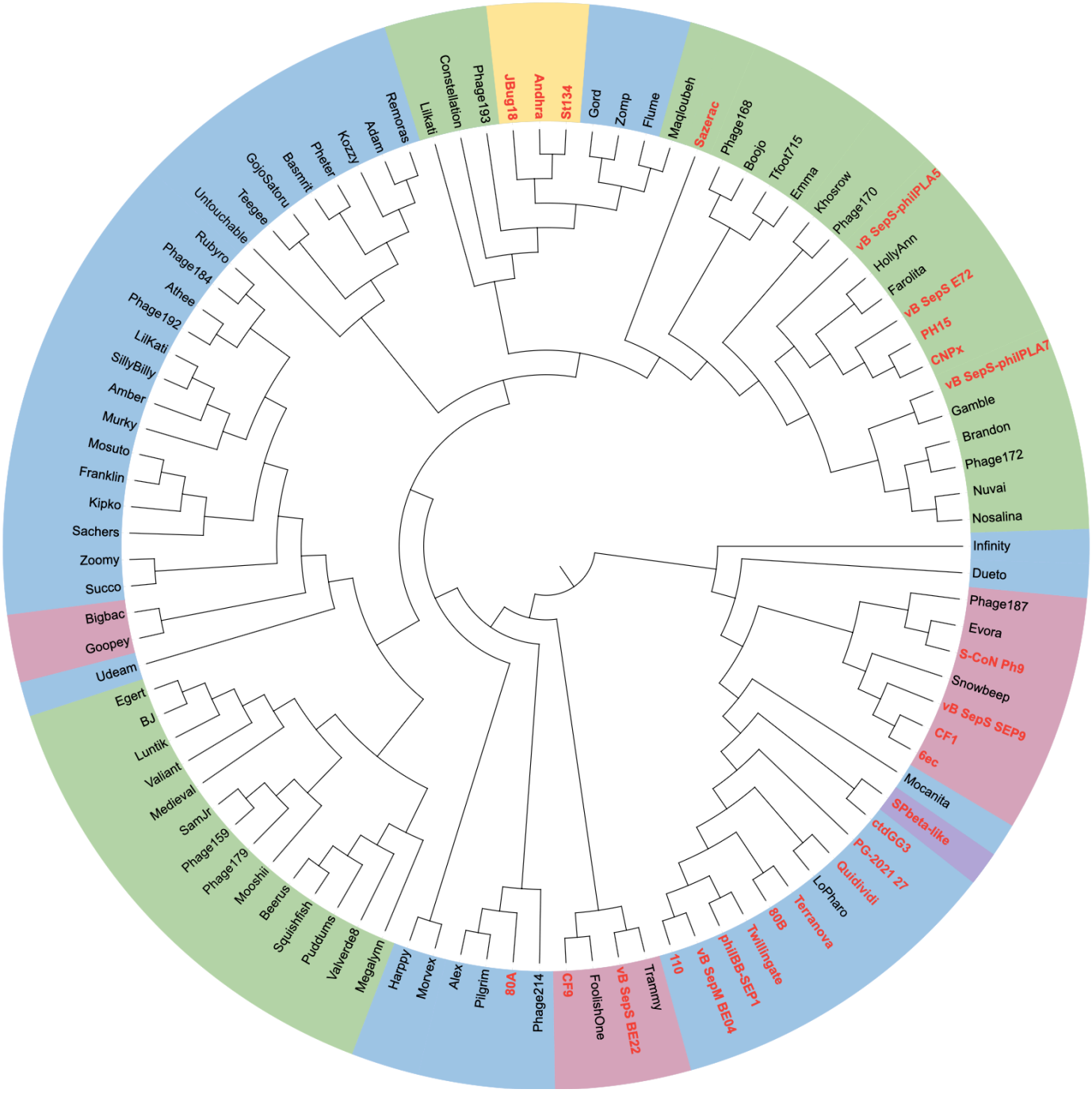

Figure 4. Phylogenetic Relationships Among *S. epidermidis* Bacteriophages. Phylogenetic tree was constructed using the neighbour-joining method based on nucleotide sequence similarity by PhageScope software and visualized using iTol software (45, 46). Phages are colour coded by predicted cluster assignment: cluster A (yellow), cluster B (green), cluster C (blue), cluster D (pink), singleton (purple). Phages shown in red represent reference genomes from established collections.

3.3 – Characterization of *Staphylococci* Bacteriophages for Phage Therapy

We aimed to narrow our follow-up study to a small and diverse collection of phages with high potential for use in phage therapy. Ten phages from this collection were selected based on the following criteria: 1) their ability to attain and retain a high titer, 2) genomic diversity, 3) preliminary host-range data, and 4) presumed fully lytic activity. This subset includes Cluster C phages Morvex, Pheter, Mosuto, Mocanita, Kozzy, LoPharo, and Cluster D phages Snowbeep, BigBac, Goopey, and Trammy. This subset of phages is the primary focus of the downstream experiments described below.

3.3.1 –Staphylococcal phages exhibit varying host range

In conjunction with the 2024 and 2025 TMM3009 lab course and Celina Tanbari, we have tested the host range of 50 phages in the collection against 12 *Staphylococcal* hosts (Figure 5). Phages with strong infectivity (red) against ≥ 3 additional strains are the most promising candidates for further study. GojoSatoru, Mosuto, Morvex, Mocanita, BigBac, Goopey, Athee, and Franklin have the broadest host range, and infect ≥ 3 additional strains (Figure 5). TerrificDeevaz, Trammy, LoPharo, Basmrit, and Mocanita also infect several hosts. By contrast, LilKati, Valient, Medieval, Farolita, HollyAnn, and Mooshii only infect their isolation host and are likely less suitable for phage therapy (Figure 5). A phenomenon called ‘killing from without’ is observed in some cases, where the abundance and high MOI can allow the phage to kill bacteria without DNA injection or phage replication (57). This activity is determined by the lack of individual plaques on a diluted spot. This is denoted as “potential infection” and is observed among several phages with broad infectivity. Figure 6 displays the host range of phages in the subset of interest; Morvex, Mocanita, LoPharo, Kozzy, Pheter, Mosuto, Snowbeep, Trammy, Goopey, and BigBac.

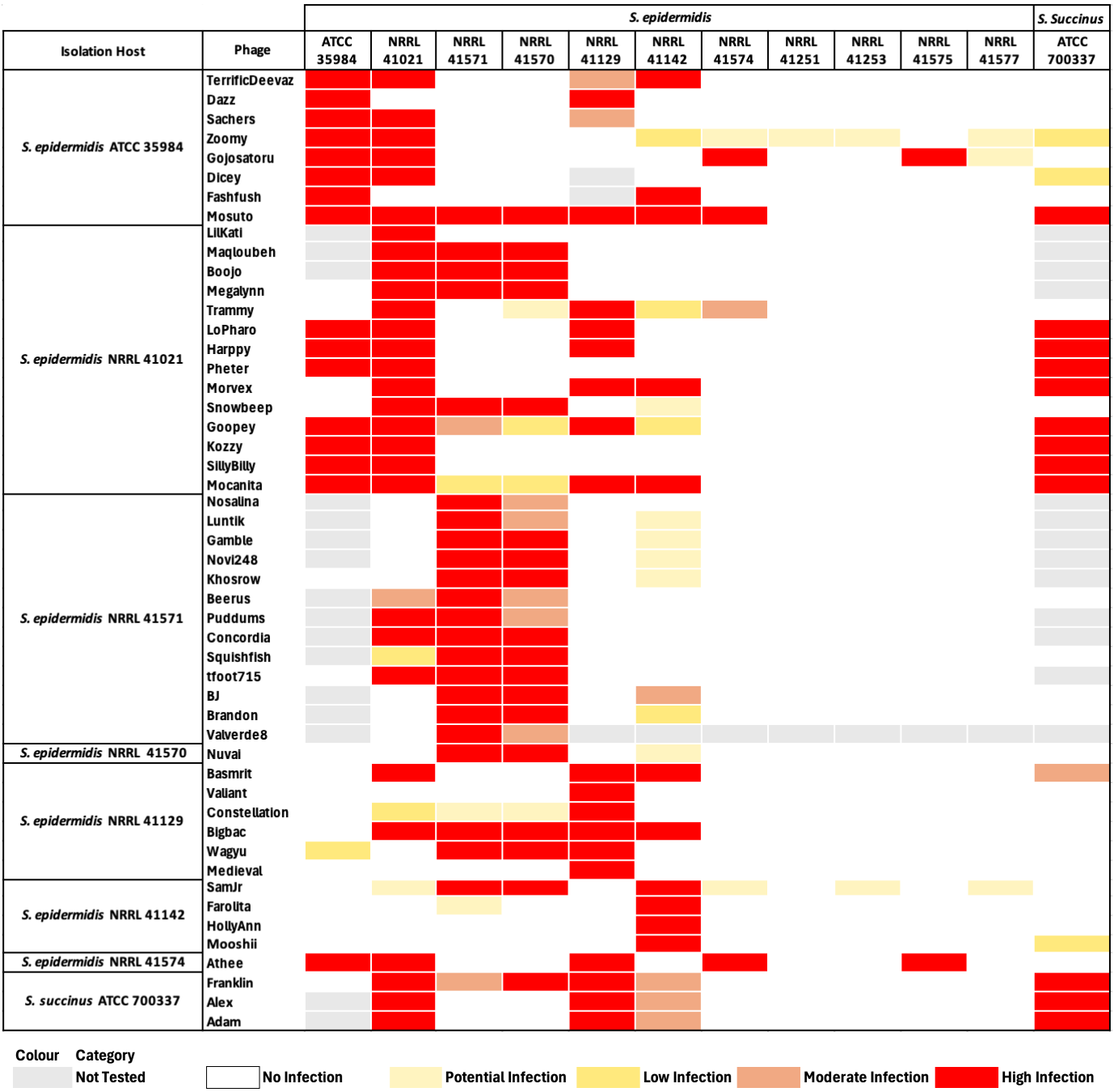

Figure 5. Heat Map of *Staphylococcal* Phages Host Range. 5 µL of *S. epidermidis* phages were serially diluted and spotted onto lawns of 11 *S. epidermidis* and 1 *S. succinus* strain in 10-fold serial dilutions from 10^{-1} to 10^{-6}. Heat map compares efficiency of plating (EOP) phage on each host.

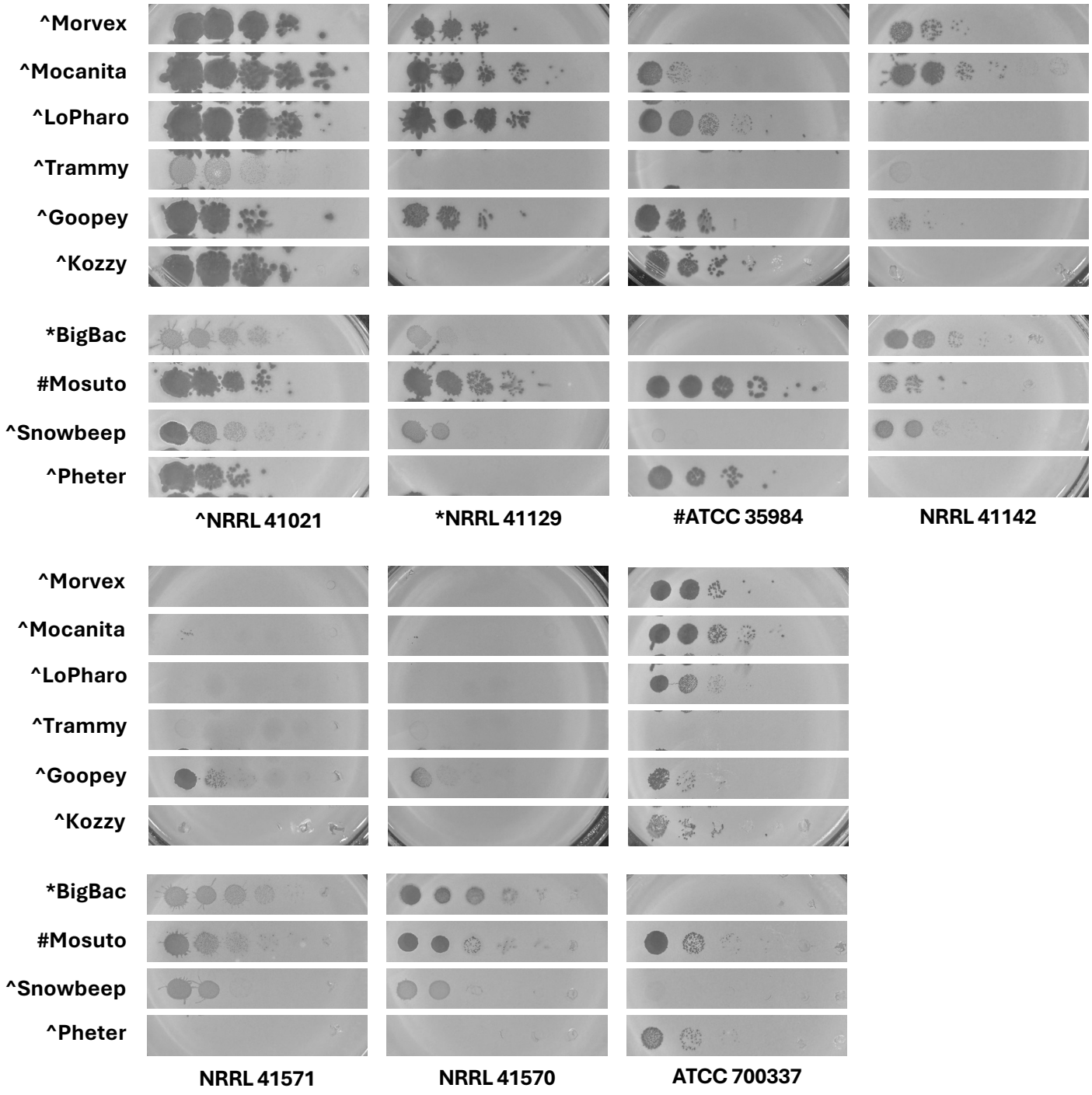

Figure 6. Host Range of *S. epidermidis* Phages Subset. 5 μL of *S. epidermidis* phages Morvex, Mocanita, LoPharo, Trammy, Goopey, Kozzy, BigBac, Mosuto, Snowbeep, and Pheter were serially diluted and spotted onto lawns of 11 *S. epidermidis* and 1 *S. succinus* strain in 10–fold serial dilutions from 10^{-1} to 10^{-6}. Phages included were from the same experimental plates, but with phages not in the subset removed. Symbols indicate isolation host: ^ NRRL 41021, * NRRL 41129, # ATCC 35984.

3.3.2 –Analysis of Staphylococcal strains in planktonic growth assays

Planktonic *Staphylococcal* growth was assessed by liquid growth assays, where cultures were grown in a 96-well plate with continuous orbital shaking and data was acquired by spectrophotometer every 15 minutes. The growth curve constructed from this data allows for comparative analysis of growth phases and growth rates of each strain (Figure 7). The growth of 10 *S. epidermidis* strains and 1 *S. succinus* strain was measured in this assay. All strains demonstrated a lag phase occurring within the first hour of growth, from OD600 0.1 to OD600 0.3. The exponential phase occurs between 1 and 6 hours at which time growth plateaus at OD600 ~1-1.4, with the exception of NRRL 41571 and NRRL 41570, which reach a peak of OD600 ~0.8. After 10 hours, the density of some strains begins to fall.

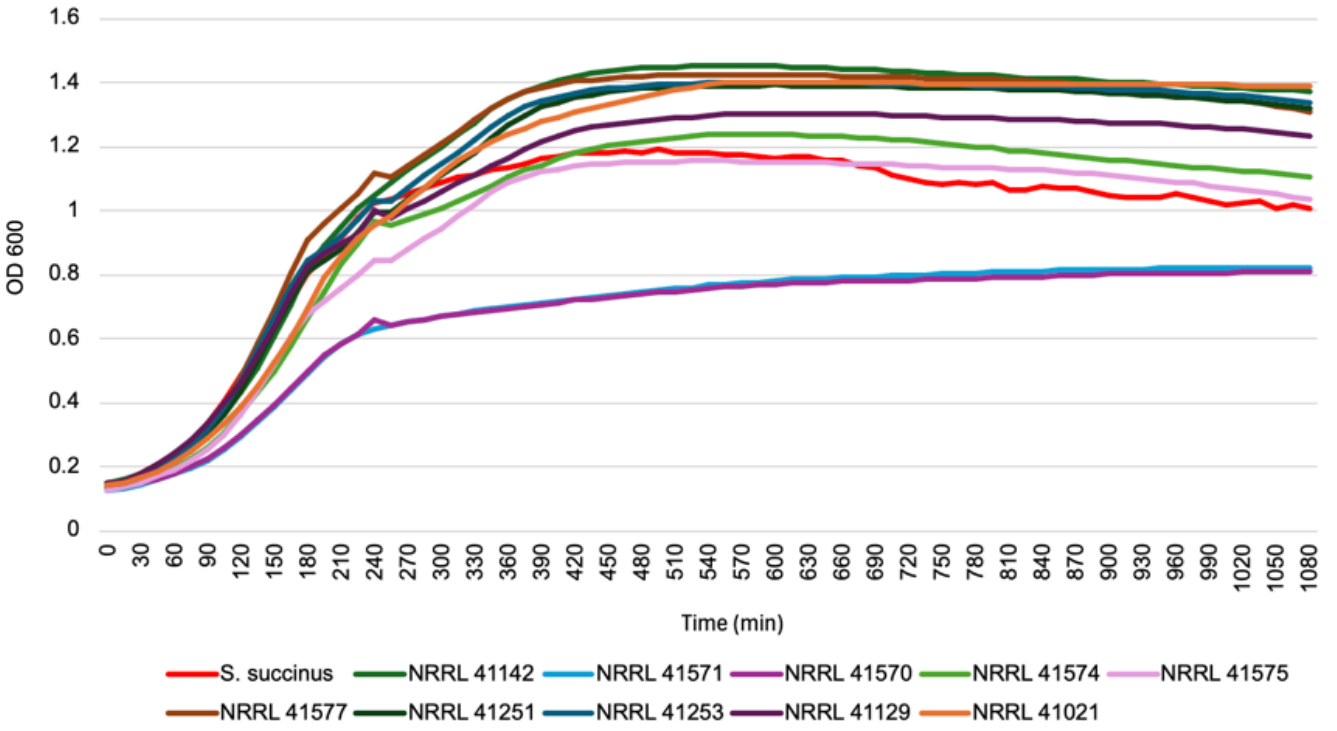

Figure 7. *Staphylococcal* Strains Growth Curves. *Staphylococcal* cultures were grown from OD600 of 0.1 in 96-well polystyrene plates over 18 hours at 34º under continuous shaking in a Bioscreen C plate reader. Each point on the curve represents the average of four replicates.

3.3.3 –Phages are effective in reducing S. epidermidis in planktonic killing assays

We tested the lytic activity of phages infecting *S. epidermidis* in planktonic growth assays, where phage is added to a bacterial culture at OD600 0.1 at varying MOIs: 0 (indicated as ctrl), 0.1, 1, 10, and 100. Relative killing ability is observed among the ten phages of interest (Figure 8A, 8B) and 1 temperate Cluster B phage (Figure 8C). Cluster C phages Mocanita, Morvex, LoPharo, Kozzy, and Mosuto, and Cluster D phages Goopey and BigBac demonstrate strong efficacy in killing or suppressing bacterial growth at most MOIs, with incomplete suppression at an MOI of 0.1, and some late-stage recovery of the bacterial culture in some cases. The relative lytic efficiency of killing can be compared between these phages, where BigBac is observed as the fastest killing, suppressing bacterial growth at most MOI's, within the first 200 minutes, Kozzy and Goopey suppress within the first 300 minutes, and other phages take even longer. By contrast, Cluster C phage Pheter and Cluster D phage Trammy may only be effective at MOI 10 or 100, and Cluster D phage Snowbeep and Cluster B phage Megalynn are unsuccessful at suppressing bacterial growth at any concentration. The recovery of the bacterial culture when treated with Megalynn is attributed to its lysogenic capabilities, which may explain the faster recovery at higher MOIs.

A

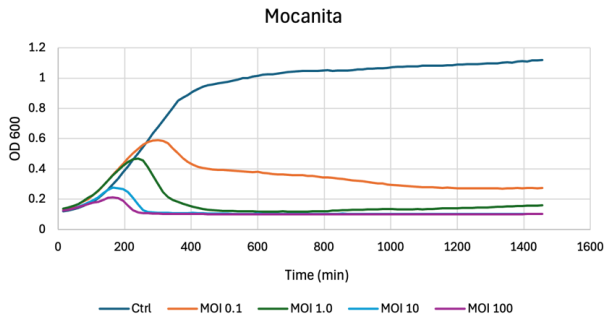
Mocanita
OD 600
Time (min)
Ctrl
MOI 0.1
MOI 1.0
MOI 10
MOI 100

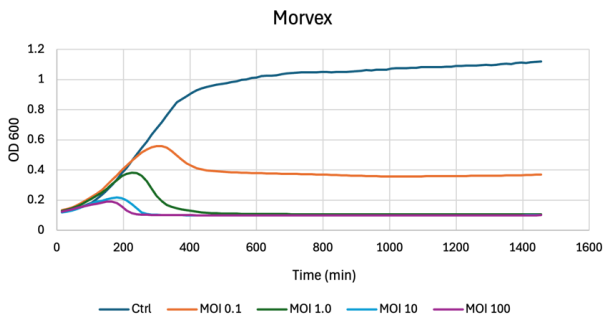
Morvex
OD 600
Time (min)
Ctrl
MOI 0.1
MOI 1.0
MOI 10
MOI 100

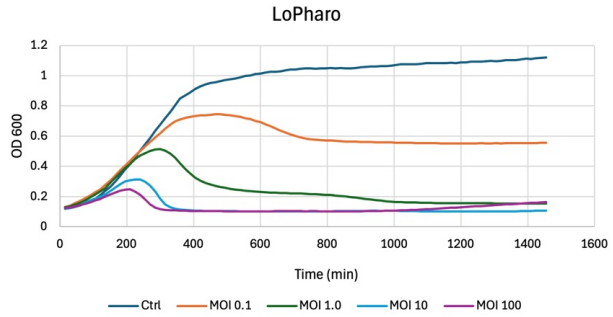
LoPharo
OD 600
Time (min)
Ctrl
MOI 0.1
MOI 1.0
MOI 10
MOI 100

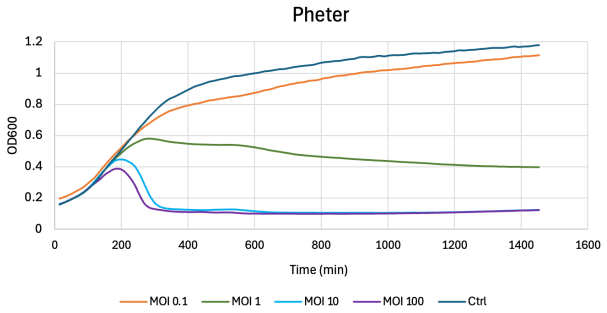
Pheter
OD600
Time (min)
MOI 0.1
MOI 1
MOI 10
MOI 100
Ctrl

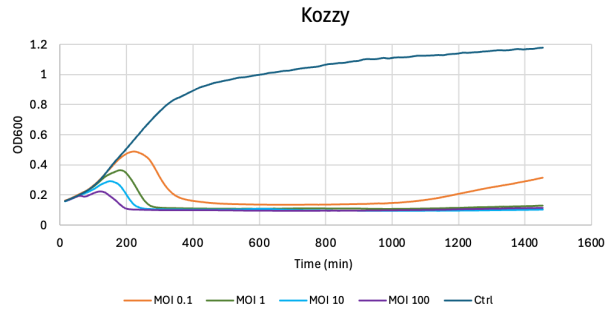
Kozzy
OD600
Time (min)
MOI 0.1
MOI 1
MOI 10
MOI 100
Ctrl

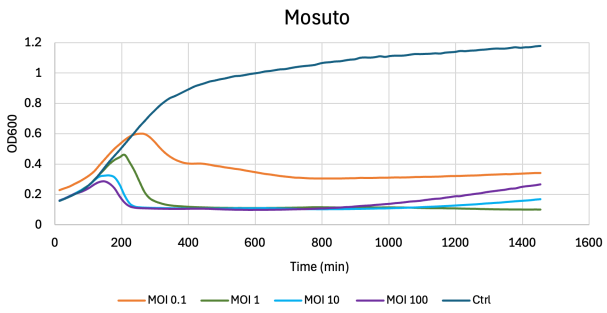
Mosuto
OD600
Time (min)
MOI 0.1
MOI 1
MOI 10
MOI 100
Ctrl

B

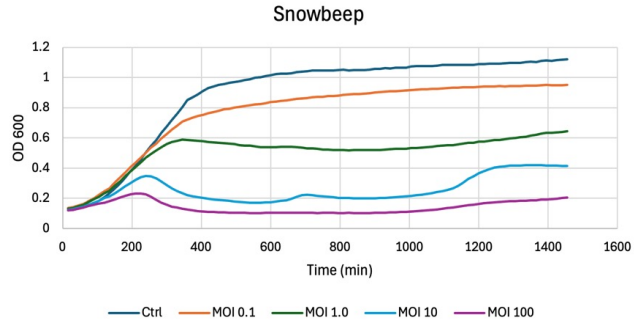
Snowbeep
OD 600
Time (min)
Ctrl
MOI 0.1
MOI 1.0
MOI 10
MOI 100

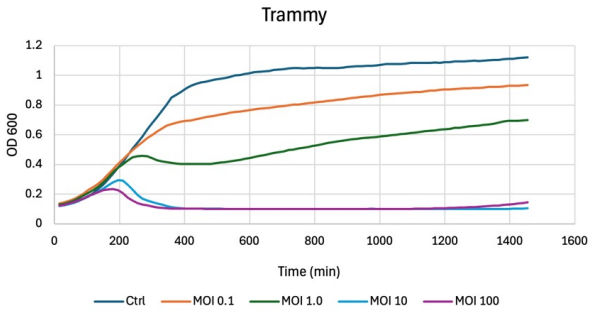
Trammy
OD 600
Time (min)
Ctrl
MOI 0.1
MOI 1.0
MOI 10
MOI 100

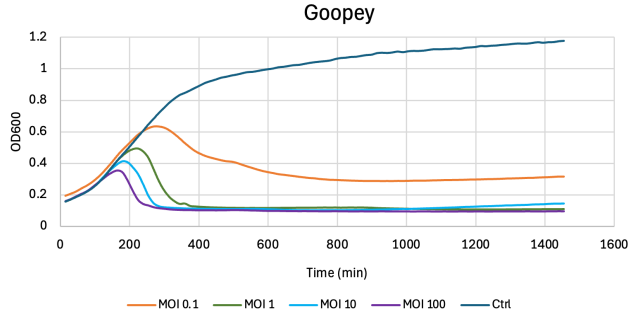
Goopey
OD600
Time (min)
MOI 0.1
MOI 1
MOI 10
MOI 100
Ctrl

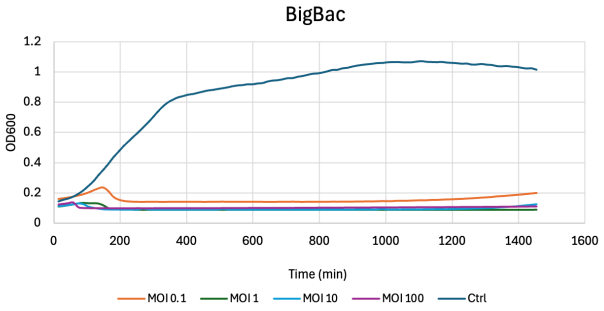
BigBac
OD600
Time (min)
MOI 0.1
MOI 1
MOI 10
MOI 100
Ctrl

C

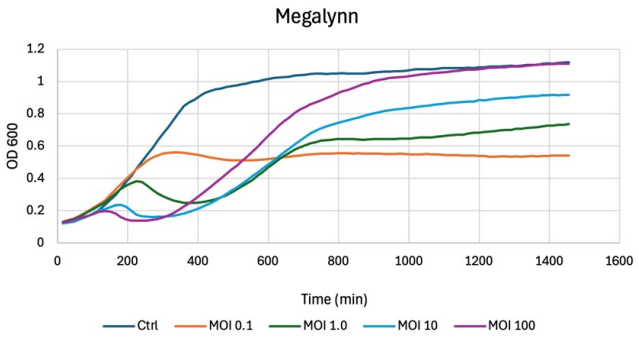

Figure 8. *S. epidermidis* Liquid Growth Curves with Phage. *S. epidermidis* NRRL 41021 cultures were grown from OD600 0.1 in 96-well polystyrene plates over 24 hours at 34º under continuous orbital shaking in a BioTek Gen 5 Microplate Reader. Phages were added at T=0 at MOIs of 0, 0.1, 1, 10, and 100. Each point on the curve represents the average of three replicates. Ctrl indicates negative control with host. **A.** Growth curves of Cluster C phages Mocanita, Morvex, LoPharo, Pheter, Kozzy, and Mosuto. **B.** Growth curves of Cluster D phages Snowbeep, Trammy, Goopey, and BigBac. **C.** Growth curves of Cluster B phage Megalynn.

3.3.4 –Staphylococcal strains exhibit varying efficacy in forming biofilms

Biofilm formation is a hallmark of *S. epidermidis* virulence, and I have tested 11 of the 13 strains for their ability to form robust biofilms (Figure 9). While variable biofilm-forming ability was observed among most strains, ATCC 35984 formed the most robust biofilm. Biofilm formation was observed in all strains relative to the media-only control, however these biofilms were not as thick and even across the bottom of the well when compared to that of ATCC 35984. This strain has been shown to form dense biofilms and is clinically relevant for orthopaedic infection experiments (17, 58, 59).

In an effort to improve experimental conditions for biofilm formation by our phage isolation strains, several optimizations were explored. As most phages of interest were isolated on NRRL 41021, this strain was most heavily pursued in subsequent experiments. While all 11 strains tested demonstrated the ability to form biofilms on polystyrene plates, all strains, except ATCC 35984, appeared to form weaker and thinner biofilms. In particular, some flakes were observed to detach during several experiments. *S. epidermidis* biofilms are time sensitive, and limitations in nutrient supply may eventually trigger detachment (17). To explore this hypothesis, a time course experiment was performed with ATCC 35984, NRRL 41021, and ATCC 700337 to assess the optimal length of time for biofilm growth (Figure 10). The *S. succinus* strain was also tested as this species is also known to form biofilms which may be infected by *S. epidermidis* phages. *S. epidermidis* biofilms are most often grown for 16–18 hours or 24 hours (58-60). Thus, biofilm growth was assessed over 12, 16, 18, 24, and 30 hours (N=4 technical replicates) and stained with 0.1% crystal violet (Figure 10). No significant difference was observed between replicates at the different time points in any of the strains, and previous issues persisted, with NRRL 41021 unable

to form strong and consistent biofilms. These results suggest that there is no distinct time point between 12–30 hours that produces a more robust biofilm.

To explore alternatives to polystyrene plates, biofilm formation was also tested on glass beads placed within wells. Glass beads provide greater surface area for biofilm growth, which is hypothesized to reduce detachment of the biofilm from the surface of the polystyrene plate. Additionally, this substrate permits testing of several beads in each well, where technical replicates can be more easily recorded. Several tests were performed to determine if this alternate substrate may support stronger biofilm formation, however similar detachment and poor biofilm formation was observed.

Thus, all phage-biofilm experiments in Chapter 3.3.5 and 3.3.6 used a TSB growth medium and were performed over 18–24 hours within the wells of polystyrene plates.

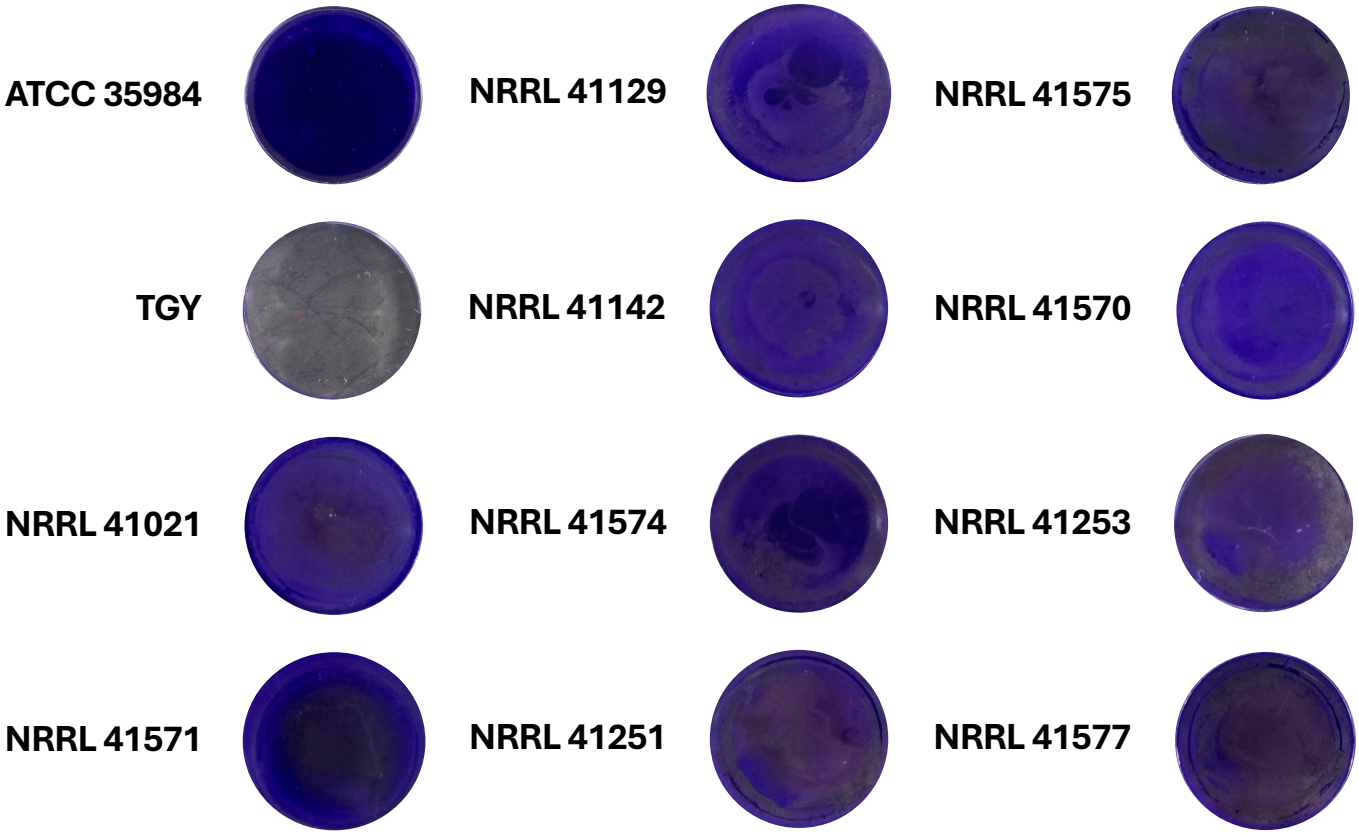

Figure 9. Biofilm Formation by *S. epidermidis* Strains. Biofilm formation was tested for 11 *S. epidermidis* strains, including ATCC 35984, NRRL 41021, NRRL 41571, NRRL 41129, NRRL 41142, NRRL 41574, NRRL 41251, NRRL 41575, NRRL 41570, NRRL 41253, and NRRL 41577. Biofilms were formed in a 24-well plate over 18 hours at 34ºC. *S. epidermidis* biofilms were stained with 0.1% crystal violet, and imaged with a handheld camera, where purple colour indicates presence of biofilm. TGY media was used as a negative control. Note: this image was photographed with a dark background, where subsequent figures were imaged with a white background.

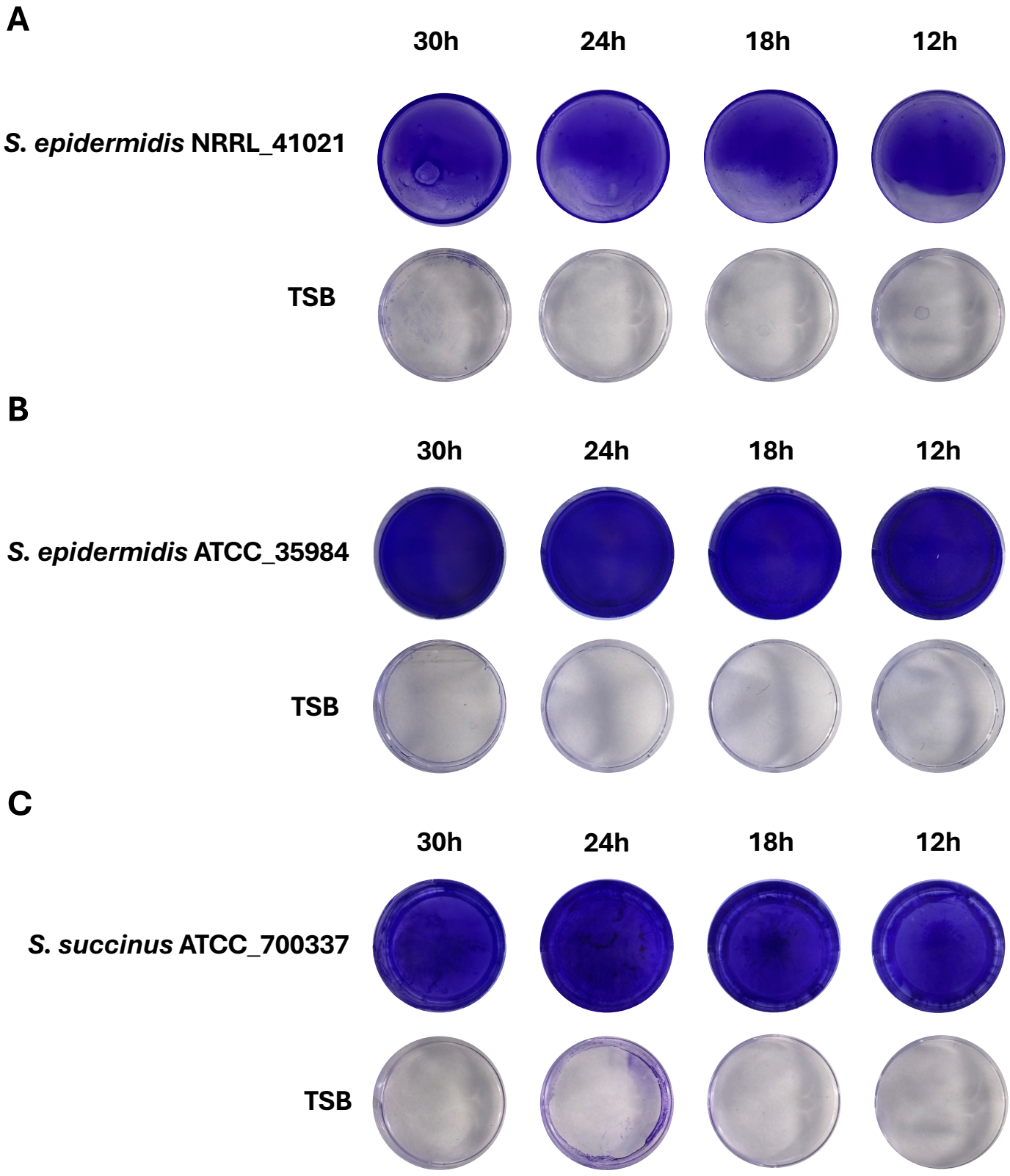

Figure 10. *Staphylococcal* Biofilm Time Course. *Staphylococcal* biofilms were formed in 24-well polystyrene plates over 12–30 hours at 34º. Biofilms were stained with 0.1% crystal violet and imaged with a handheld camera, where purple colour indicates presence of biofilm. Each condition was performed in 4 technical replicates. **A.** *S. epidermidis* NRRL 41021. **B.** *S. epidermidis* ATCC 35983. **C.** *S. succinus* ATCC 700337**.**

3.3.5 –Phages exhibit varying efficacy in inhibiting Staphylococcal biofilm formation

A biofilm inhibition assay was performed to assess the ability of the subset of phages to prevent biofilm formation by a *Staphylococcal* host. As in the planktonic growth assay, phages at varying MOIs were added with the host into polystyrene plates and biofilm was assessed 18–24 hours later. An additional phage that did not share host range to the host was included as a negative control. *S. epidermidis* NRRL 41021 and ATCC 35984, and *S. succinus* ATCC 700337 were used in these assays, as they were the isolation host of most phages of interest and/or many of the phages displayed host range on them.

Pheter, LoPharo, Trammy, and Snowbeep were highly effective at reducing biofilm formation by *S. epidermidis* NRRL 41021 when added at an MOI of 1 and 100, and all but LoPharo were effective at an MOI of 0.1 (Figure 11A). In contrast, phage Khosrow, a non-infecting control that lacks the ability to infect this host, had no disruptive effect, and similar biofilm formation occurred irrespective of the MOI of phage added. Some regions of higher bacterial density were observed in the phage-treated conditions, and we hypothesize that these may be a combination of phage-resistant cells that grow rapidly after most of the host is killed and/ or clumps of crystal violet.

Mosuto, Kozzy, Mocanita, Goopey, and Pheter were highly effective at reducing biofilm formation by *S. epidermidis* ATCC 35984 (Figure 11B). Mosuto appeared far more effective than other phages, having the least biofilm in all three treated wells, while Mocanita appeared the least effective, with much more biofilm remaining in all three treated wells, but still distinct from MOI of 0. In contrast, phage Trammy, a non-infecting control that lacks the ability to infect this host, had no disruptive effect, and similar biofilm formation occurred irrespective of the MOI of phage added. Stained cells were observed in the phage-treated conditions, suggesting that this strain may

establish biofilms rapidly, and that this strain can rapidly acquire resistance to the phage, evading phage infection.

Sachers, Morvex, Mosuto, Pheter, LoPharo, and Goopey were highly effective at preventing biofilm formation by *S. succinus* ATCC 700337 (Figure 11C). All phages appeared effective in all three treated wells, compared to MOI of 0, in particular MOI 100 appeared the most effective. Residual crystal violet stain was visible in the rim of some high MOI-treated wells, this may be attributed to improper washing of the biofilm post-staining. The negative control phage differed from biofilms of *S. epidermidis* hosts, as Sachers appeared to have an inhibitory effect on the biofilm, despite its intended use as a negative control and lacking host range to this host when tested on plates. This observation was also seen in replicates of this experiment, where other phages previously shown to lack host range displayed levels of biofilm inhibition similar to the experimental phages. Overall, the inhibition of biofilm growth observed following phage treatments supports the use of these phages in downstream biofilm destruction experiments.

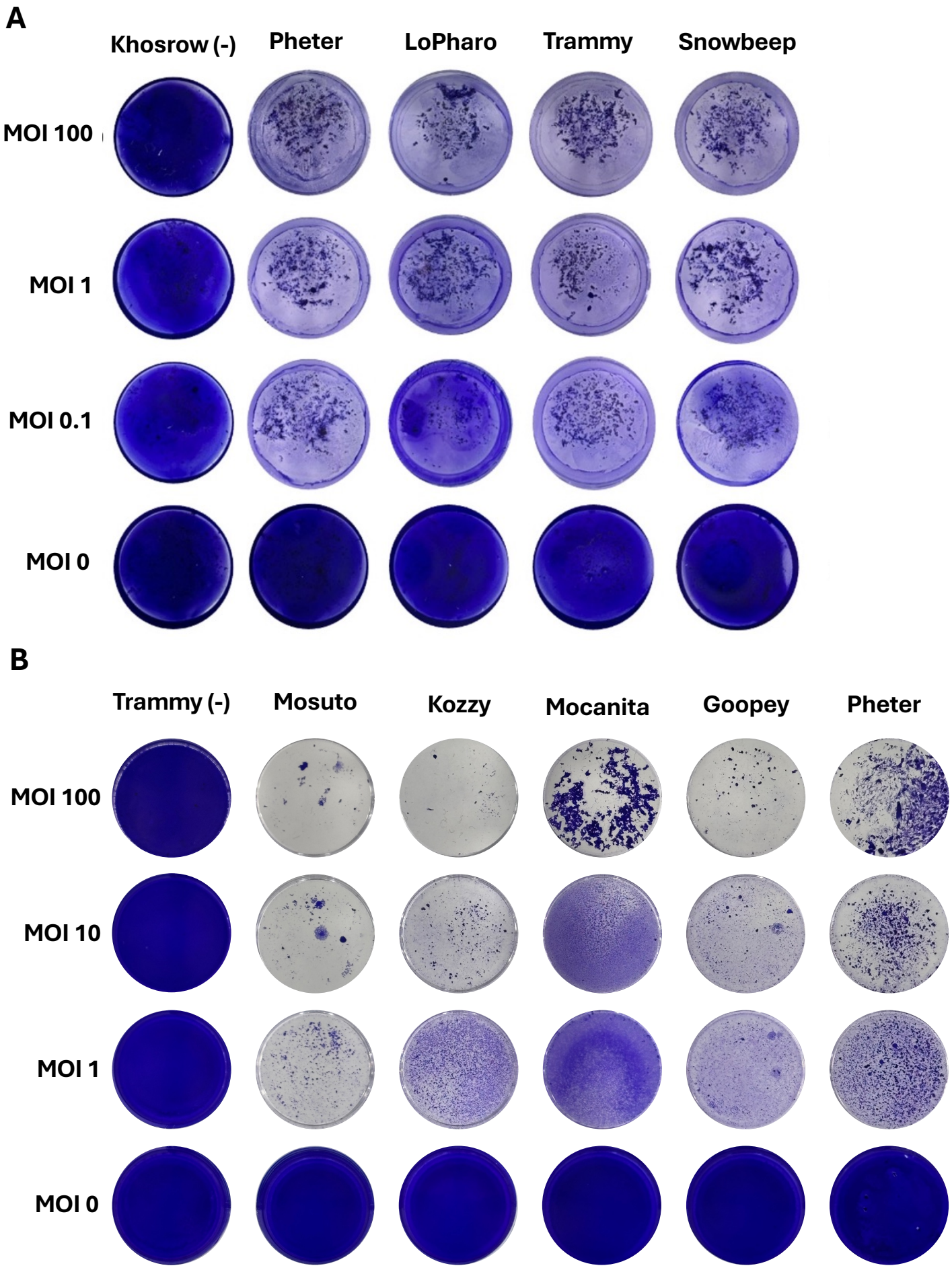
A
Khosrow (-)
Pheter
LoPharo
Trammy
Snowbeep
MOI 100
MOI 1
MOI 0.1
MOI 0
B
Trammy (-)
Mosuto
Kozzy
Mocanita
Goopey
Pheter
MOI 100
MOI 10
MOI 1
MOI 0

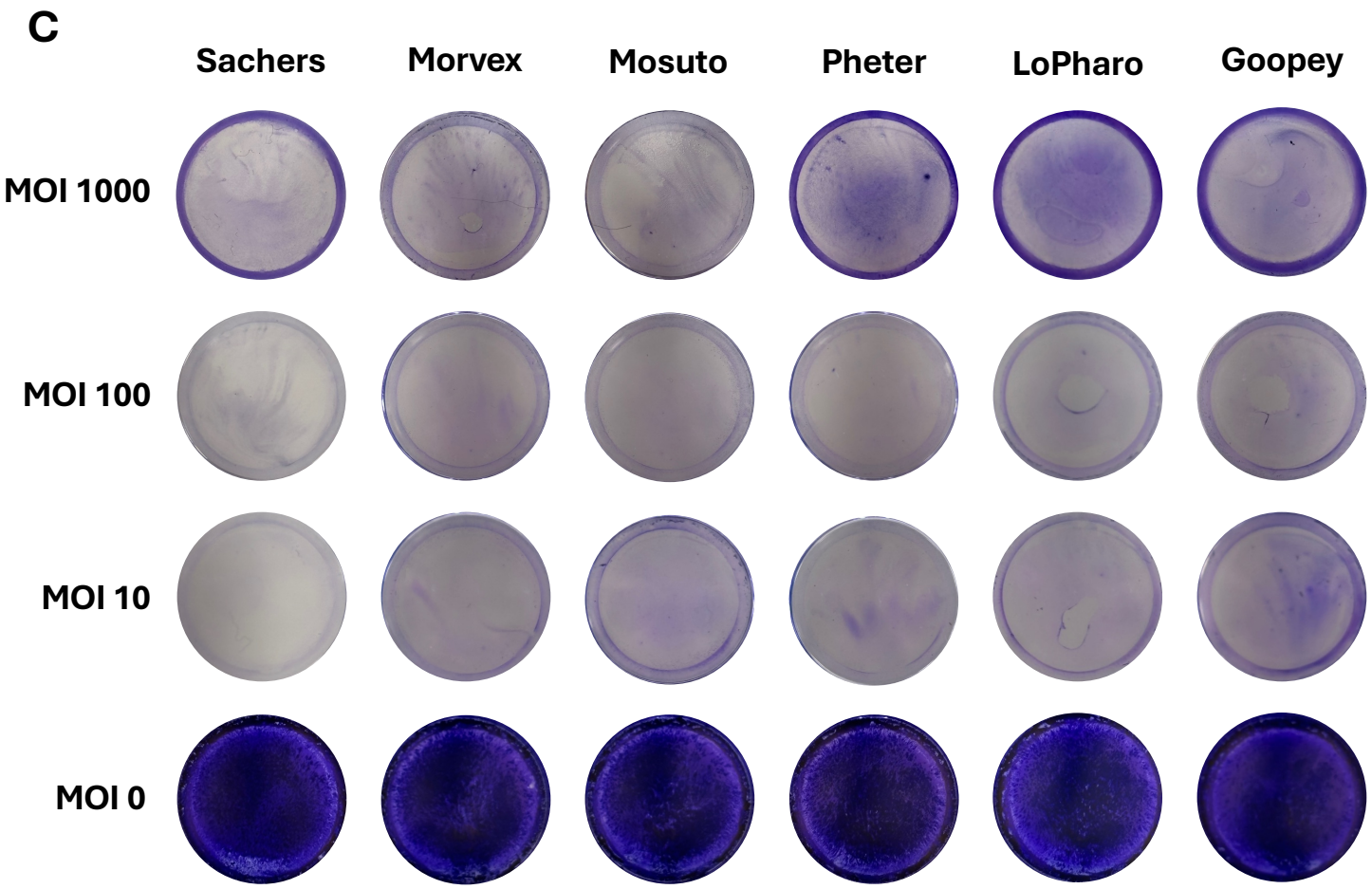

Figure 11. *Staphylococcal* Biofilm Inhibition by Phage. *Staphylococcal* biofilms were formed in 24-well polystyrene plates over 18–24 hours at 34º. Biofilms were stained with 0.1% crystal violet and imaged with a handheld camera, where purple colour indicates presence of biofilm. (-) Indicates phage that does not infect the host. **A. *S. epidermidis* NRRL_41021.** Phages Khosrow (-), Pheter, LoPharo, Trammy, and Snowbeep at MOI from 0 to 100. Note that crystal violet used in this replicate was not recently filtered and is partially attributed to the presence of clumps seen throughout each well. **B. *S. epidermidis* ATCC_35984.** Phages (left) Trammy (-), Mosuto, Kozzy, Mocanita, Goopey, and Pheter (right) at MOI from 0 to 100. **C. *S. Succinus* ATCC_700337.** Phages Sachers, Morvex, Mosuto, Pheter, Lopharo, and Goopey at MOI from 0 to 1000.

3.3.6 –Phages exhibit low efficacy in disrupting Staphylococcal biofilm formation

The biofilm destruction assay was performed to observe the ability of phages in the collection to destroy 24–hour pre-formed biofilms. This experiment better models what may occur in phage therapy, where phages would be administered against a pathogen that had already formed a biofilm in a prosthetic joint. These experiments were performed with varying MOIs of phage, relative to the concentration of the initial bacterial inoculum, alongside an MOI of 0 negative control, and a non-infecting phage control. *S. epidermidis* NRRL 41021 and ATCC 35984, and *S. succinus* ATCC 700337 were used in these assays, as they were the isolation hosts of most phages of interest and/or many of these phages displayed host range onto them. Biofilm destruction experiments on *S. epidermidis* NRRL 41021 were unsuccessful, as biofilms appeared to detach in treated and untreated wells during the addition of phage and washing steps as described in Chapter 3.3.4, preventing analysis.

Mosuto, Kozzy, Mocanita, Goopey, and Pheter, did not successfully reduce or destroy a 24–hour biofilm formed by *S. epidermidis* ATCC 35984 (Figure 12A). Based on results from several previous attempts, MOIs up to 1000 were tested in this assay. However, no observable difference was visible between treated and untreated controls, and these phages showed no effect on the biofilm.

Trammy, Mosuto, Kozzy, Mocanita, Goopey, and Pheter were effective in reducing a 24–hour biofilm formed by *S. succinus* ATCC 700337 (Figure 12B). Higher MOIs were also used in this experiment. A difference was observed between MOI 1000 and the untreated MOI of 0 control, but only marginal effects were observed at MOI 100 and 10.

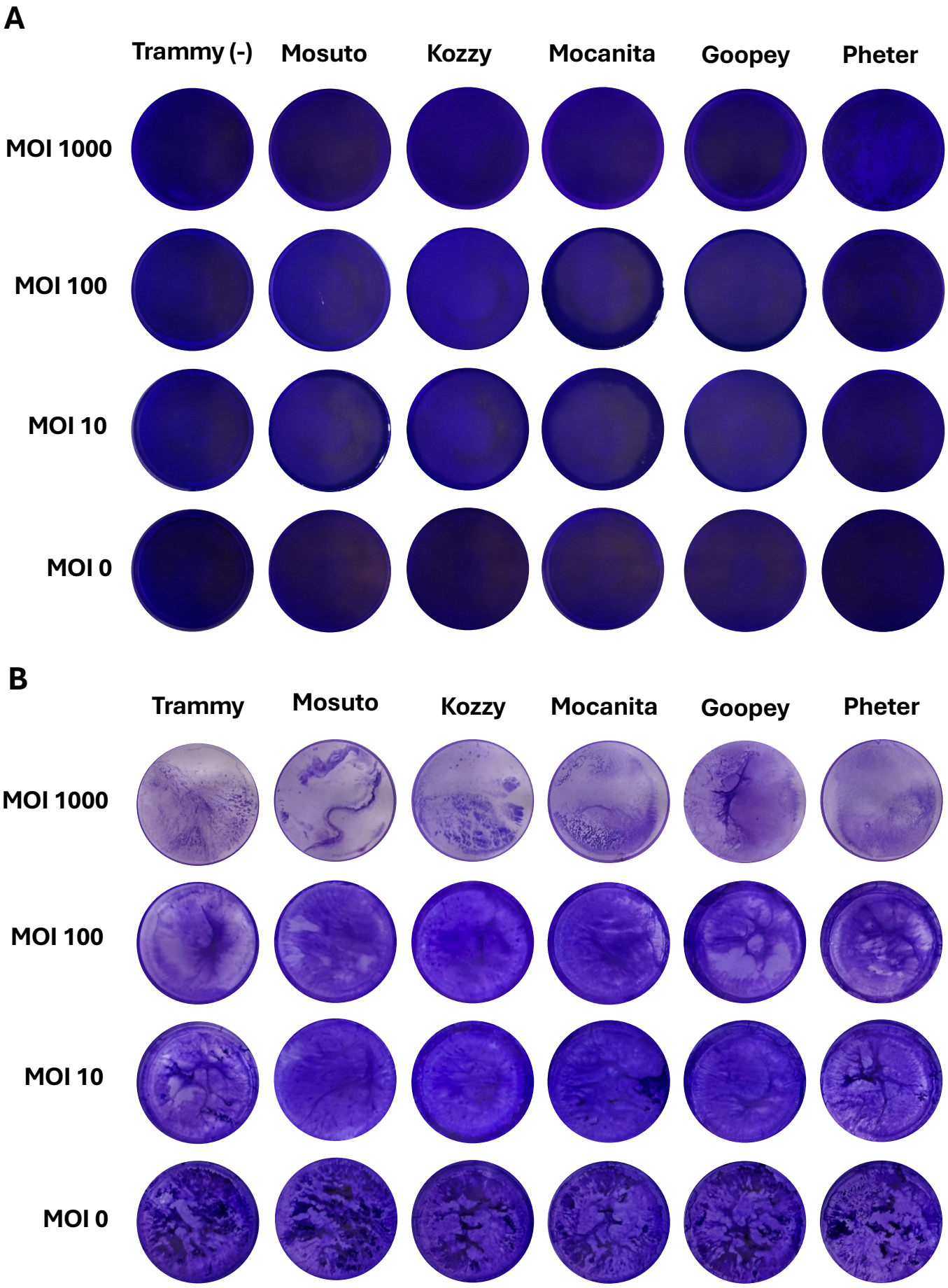
A
Trammy (-)
Mosuto
Kozzy
Mocanita
Goopey
Pheter
MOI 1000
MOI 100
MOI 10
MOI 0
B
Trammy
Mosuto
Kozzy
Mocanita
Goopey
Pheter
MOI 1000
MOI 100
MOI 10
MOI 0

Figure 12. *Staphylococcal* Biofilm Destruction by Phage. *Staphylococcal* biofilms were formed in 24-well polystyrene plates over 18–24 hours at 34º. Planktonic bacteria were removed and phage was added at a theoretical MOI relative to the concentration of the initial inoculum. Biofilms were stained with 0.1% crystal violet and imaged with a handheld camera, where purple colour indicates presence of biofilm. (-) Indicates phage that does not infect the host. **A. *S. epidermidis* ATCC_35984.** Phages Trammy (-), Mosuto, Kozzy, Mocanita, Goopey, and Pheter at MOI from 0 to 1000. **B. *S. Succinus* ATCC_700337.** Phages Trammy, Mosuto, Kozzy, Mocanita, Goopey, and Pheter at MOI from 0 to 1000.

Chapter 4 – Discussion

4.1 – *S. epidermidis* Strains are Viable for Phage Work

4.1.1 – Phage activity reflects host strain growth conditions

The successful isolation of bacteriophages infecting *Staphylococcus epidermidis* required careful optimization of host strains, as host growth conditions are critically involved in phage-host interactions, and may influence the type of phages isolated. As described in Chapter 2, several optimizations were made to improve bacterial growth conditions, particularly in the TGY agar used. The exclusion of K_2HPO_4 from TGY agar was decided based on repeated cloudiness in the agar, leading to concerns of contamination, lack of reproducibility, and concern of the impact of potential peroxide on damaging host growth or phage particles. No negative change was observed in phage activity following this change, and agar appearance was consistent. The choice to drop agar concentration in the top agar from 0.4% to 0.3% was intended to enhance phage diffusion through the soft agar, promoting phage adsorption and burst size, allowing for a greater number of more easily identifiable plaques. TSB media was used for biofilm experiments, where greater nutrients and glucose are required for supplementing growth of strong bacterial biofilms. The decision to perform experiments at 34ºC rather than the isolation temperatures denoted for the strains by NRRL and ATCC, was chosen to provide consistency in the conditions that phages were being tested under, and to emulate the natural skin temperature. Additionally, 34ºC was considered a "happy medium" between the recommended temperatures provided, ranging from 28º–37ºC. In some instances, where strains were unsuccessful in isolating phage, growth at 30ºC and 37ºC were explored, however no change in the appearance of the lawn or phage isolation success occurred. In hindsight, growth at 37ºC may have been more optimal for making experiments most clinically

accurate, as this would most resemble the temperature inside the body, the environment phages would be used in in a true phage therapy application.

4.1.1 – Diversity within phage collection reflects diversity in isolation hosts

A diverse panel of 14 *Staphylococcal* strains was used to maximize diversity of phages isolated (Table 1). Majority of these strains are not genome sequenced, limiting ability to compare aspects that might impact phage predation. We postulate that some variation exists in their surface receptors and potential defence machinery governing their susceptibility to different phages. This is especially important as *Staphylococcal* phage host range, is often quite narrow, thus generating a broad collection of phages infecting different hosts is of importance.

Additionally, while use of BSL-1 strains allows greater safety and reproducibility in the work, they may pose some limitations. Phage hunting exclusively on BSL-1 strains may restrict the selection of phages found, as more strains that virulent and clinically relevant may possess resistance genes and defence mechanisms that impede phage predation, thus may only be infected by a more 'robust' set of phages, and must be hunted for explicitly. With the exception of ATCC 35984, by primarily using these non-clinical strains, that likely do not have strong phage defence, we may be selectively isolating the 'easy to find' phages. This may explain the lack of ability to find phages on NRRL 41251, NRRL 41253, NRRL 41575, NRRL 41577, NRRL 4268, and NRRL 2616, as these strains may have stronger defence systems and require more rigorous isolation sample types.

Additionally, our intentions behind isolating and amplifying phages on *S. succinus* were successful, where the 8 phages found appear to have similar diversity as *S. epidermidis*–isolated phages, and were found to have strong host range onto the *S. epidermidis* strains (Figure 5). *S. epidermidis* and *S. succinus* are both CoNS species with similar phylogenetic background, and

both exist in skin environments, increasing propensity for horizontal gene transfer. Thus, genetic overlap and conserved elements, including surface receptors, is highly likely. Additionally, both species are opportunistic pathogens and share similar clinical infection types, though *S. epidermidis* clinical isolates are generally more virulent.

We believe using diverse hosts allowed us to find a more diverse set of phages. This is reflected in Chapter 3.2 and will be discussed further in Chapter 4.2.

4.1.3 – S. epidermidis strains have variable success in phage isolation

79 phages infecting *S. epidermidis* were sequenced and/or archived through this isolation pipeline, with near 100 total phages found (Table 2). These results surpass totals of *S. epidermidis* phages described in major studies by Oliveira et al., and Lopes et al. (34, 40). Sampling from a large set of volunteers with a strong emphasis on improving our sampling methods throughout the study was a large factor attributed to the isolation success.

Variability was observed in the success of isolation host strains used, where some had great success and thus were tested more frequently, unsuccessful hosts were less frequently tested. Some preliminary testing of non-skin-swab isolation samples was performed for these unsuccessful strains including filtered samples of sewage and influent, and from several types of beer (mirroring the original isolation host of NRRL strains 41251 and 41253), however these attempts were also unsuccessful in finding phage. We hypothesize that there may be internal defences or prophages within these strains that protect the bacteria from phage predation. These strains must be sequenced to properly examine this hypothesis, however for the scope of this study we focused initially on strains with high success rates.

Additionally, the workflow used in this project isolated and tested phages primarily against laboratory strains of *S. epidermidis* which are largely avirulent. We hypothesize that the diversity

of the collection may differ if phage isolation was performed directly on clinical isolate strains. Some studies have described a successful methodology using clinical isolates to phage hunt, and in these successful cases, the phage found is highly effective against its host, compared to one isolated on a reference strain.

A study by Ferriol-González and colleagues demonstrated efficacy of a targeted phage hunting method on *Klebsiella pneumoniae* clinical isolates, where the phages found directly on these isolates were far more effective than a cocktail of phages isolated on reference strains (61). They denote this method as faster and more effective for targeting a particular isolate, highlighting that many clinical isolates have phage defence mechanisms which prevent infection of a high proportion of phages. Further they recommend the use of reference strains for testing cross-infection and use for propagating particular phages found on an isolate of interest.

Some limitations prevent this from being feasible for this project: these clinical strains are often more virulent with potential to be pathogenic thus require higher biosafety and ethical considerations to perform work with them, additionally, clinical isolate strains may be more difficult to culture and perform reproducible work. As a result, for the scope of this project, testing phage discovery on BSL-1 *S. epidermidis* strains was the most effective method to ensure success in finding and characterizing phages for this project.

4.1.4 – Phage morphotype is elucidated through transmission electron microscopy

One notable discovery occurred in the identification of contractile and extended tail morphologies of the Myoviruses through TEM images (Figure 1, 2). Generally, the contractile tail machinery should only become active when infecting a bacterial cell, thus this observation in the absence of a bacteria is unexpected. We postulate that conditions within the phage lysate are responsible for triggering this contraction, however further work is required to understand the

cause. This observation may have had implications in other areas of this work, where we have observed that the infectious titers calculated off these lysates rapidly drop over time. This may be a result of this spontaneous contraction over time, leaving phages unable to infect the host when used months later. Comparison of filtered plate lysates to more purified phage preparations such as cesium chloride treatment, may allow us to determine if spontaneous contraction is an intrinsic property of these Myoviruses, or if components of the plate lysate trigger tail contraction.

As noted in Chapter 3.1.3, 26 phages in the collection were not imaged or were poorly imaged. In these cases, grid preparation was optimized in several ways, as described in Chapter 2.8. A large majority of these instances were due to difficult-to-amplify phages, where in some cases PEG precipitation was explored to generate high titer lysate. Additionally, for phages of 10^7 – 10^8 pfu/mL, just below the recommended 10^9 pfu/mL, longer incubation on the grid may be sufficient to improve chances of phages adhering to the grid. In cases where imaging was performed but a poor image was achieved, nuclease treatment, PEG precipitation, and use of Tween 20 detergent was effective at improving staining of the grids to achieve better contrast between the negatively stained phage and the grid. Background noise was successfully reduced as compared to previous imaging attempts.

4.2 – *Staphylococci* Bacteriophages Can Be Clustered and are Genomically Diverse

4.2.1 – Direct-from-plaque sequencing is effective, but has some pitfalls

The direct-from-plaque Nanopore Sequencing was the most robust and efficient method used, generating several complete genome sequences (Figure 3). This method has completely changed our phage isolation pipeline, where phages may now be sequenced directly following their isolation, and the sequence may be used to determine if the phage is worth pursuing. In the context of creating a collection of phages for therapy, Cluster B phages whose sequence matched to a bacterial host sequence were discarded, and phages which had strong matches to Cluster A, C, or D phages, especially those which appeared more unique, were prioritized for downstream work.

However, this method has some drawbacks which may need to be resolved to improve its efficacy and before relying solely on this method for whole-genome sequencing. Primarily, the human error involved in manual plaque picking for obtaining phage DNA often results in accidental sequencing of the host bacteria. Having genome sequenced hosts will allow the removal of these reads during genome assembly, which can allow full genome assembly. Additionally, we are testing if picking from a "webbed" plate, rather than a single plaque may increase the ratio of phage to host genome reads. Additionally, resultant sequence lengths were quite variable between Nanopore runs and phages, with some runs producing several complete sequences, and others only obtaining a few hundred bp of a particular phage. In particular, Siphoviruses were found more likely to be full sequence, while full sequences of Myoviruses were unattainable by Nanopore sequencing (Table 2). This is reflective of their larger genome sizes; thus, successful sequencing of these longer genomes requires more active pores and high concentration DNA.

4.2.2 – Sequencing reveals clusters B, C, and D phages, but not cluster A

The clustering method described by Oliveira in the 2019 study was effective in comparing and categorizing sequenced phages in this collection, where clustering determination was

supported by TEM and observed lytic/ lysogenic activity. All sequenced phages were organized into clusters, though clustering determination of phages with extremely short sequences, or sequences matching to highly conserved regions should be taken into consideration. Clustering identified phages within Cluster B, C, and D, but not in Cluster A (Table 2). The lack of Cluster A phages is hypothesized to be due to sampling bias, where Cluster A phages may not generally be as prevalent on the skin and may be more likely found in other sampling types such as sewage. In contrast, the high percentage of Cluster B phages is expected from sampling as most naturally occurring *S. epidermidis* strains contain lysogens. The isolation host also largely effects what phages are found, and it may be possible that many Cluster A phages are unable to infect the hosts used in this study. While they are more limited in comparison to other clusters of *Staphylococcal* species, several studies have had success in isolating Podoviruses. In particular, a 2017 study by Cater and colleagues denotes the discovery of Cluster A phage Anhdra, which was isolated from a sewage sample on ATCC 35984, a host used in our study (62). This establishes that it is possible to find Cluster A phages on this host, and thus testing from other types of samples may be a more promising future direction.

4.2.3 – Genome comparison suggests some evolutionary diversity among the collection

The uniqueness of phages in this collection was assessed both by comparison of our phages with existing reference phages, and inter-comparison between phages in the collection. Comparison of the genome matches through NCBI blast was the primary method of determining novelty among phages in the collection to available reference phages (Table 3). In this method, a low query cover or sequence identity reveals that a phage may have some or all regions of its genome distinct from reference phages, determining their relatedness. Mocanita was one of few

phages of interest which revealed low query cover to a notable Twort-like reference phage Terranova and had high similarity to only one other partial phage sequence (Table 3).

Phylogeny was used to visualize inter-relatedness of phages in the collection and relatedness to reference phages (Figure 4). The tree comparison revealed diversity between these phages, where varying branch points separated phages within the same clusters into further groups of relatedness, suggesting evolutionary descent and potential functional differences. However, as many phages included in this tree are incomplete, and relationships will likely change when full genome sequences are used. Despite these caveats, we are intrigued by the shared node between Cluster C phages Flume, Gord, and Zomp and Cluster A reference phages, and the common node between Cluster C phage Mocanita and Singleton SPbeta-like phage. These relationships may be an example of non-linear evolution of these phages in which genome exchange events can drive phage genome evolution.

As stated previously, further phage hunting on a greater diversity of isolation hosts and broader sampling types may be required to acquire further diversity in the collection, as many phages from similar environments and found on similar hosts are expected to have high degree of relatedness. Overall, substantial genomic diversity is observed within this collection, with many phages appearing genomically unique and phylogenetically distinct. The clustering system allows for organization of the collection, supports determination of phages of interest, and highlights weak points in the collection.

4.3 – Several *Staphylococci* Bacteriophages Appear Suitable for Phage Therapy

4.3.1 – Broad host range is promising for phage therapy

Host range experiments revealed several phages with a broad host range, and we anticipate that these phages have greater potential to infect clinical isolates (Figure 5). Future experiments include testing host range onto *S. epidermidis* clinical isolates to assess our phages efficacy against more virulent strains. A prominent concern is that while many of these phages may exhibit a broad host range among laboratory strains, they may be less infectious, or entirely ineffective against an infection-causing bacteria. As ATCC 35984 is known to have phage defence capabilities, we postulate that phages which infect this strain may be more successful in infection of clinical isolates (52, 53). Six of ten phages in the subset of interest, excluding Morvex, Trammy, BigBac, and Snowbeep, were able to infect this strain (Figure 6).

4.3.2 – Liquid growth assays are useful for analyzing bacterial growth

Understanding the physiology of the host strains used in this study is extremely important in providing a baseline for understanding phage-host kinetics (Figure 7). As phage infection dynamics rely on bacterial growth phase, growth curve data outlining the growth pattern for each strain is important for future analysis. As identified in Chapter 3.3.2, lower maximal growth was observed among NRRL 41571 and NRRL 41570 (Figure 7). This may be attributed to spontaneous induction of a prophage within these strains, which could become lytic, reducing the maximal growth. Preliminary host sequencing indicates that there may be a prophage in the NRRL 41571 genome, and additionally our isolation data indicates that all 10 sequenced phages isolated from NRRL 41571 are temperate.

4.3.3 – Liquid killing assay supports analysis of phages lytic efficiency

Comparison of phage replication efficiency and lytic potency allows us to compare phages killing efficacy and can be used to detect the ability to lysogenize (Figure 8). This data elucidates

levels of lytic activity, where varying efficacy at different MOIs can rank lytic potency between phages. Further testing of promising phages at MOIs below 0.1 would be interesting to assess how much phage is truly needed for killing to occur. The differences observed in the length of time taken to kill the bacteria are attributed to differences of phage diffusion, adsorption kinetics, burst size, and latent phase, where some phages may be more successful at finding their host and faster replication, indicating greater killing efficiency. Our data suggests that phages BigBac and Kozzy may be more favourable for phage therapy, where these phages would be a faster-acting therapeutic.

4.3.4 – Not all S. epidermidis strains are strong biofilm formers

Difficulties of achieving biofilm formation for most laboratory *S. epidermidis* strains were observed in Chapter 3.3. While all strains appeared capable of forming a biofilm adhered on polystyrene plates, at some level, ATCC 35984 clearly formed stronger biofilms than other strains, like NRRL 41021 (Figure 9). As described in Chapter 2.15, optimizations to this assay included comparing static vs shaking (120 rpm), TGY vs TSB media, and media supplementation. The time course experiment was performed in attempt to determine a particular timepoint for performing the experiment, however biofilms appeared similar at all times, and no particularly effective time was identified (Figure 10). Despite this optimization, most strains still formed suboptimal biofilms. All strains, other than ATCC 35984, consistently formed biofilms with a propensity to flaking off from any agitation (i.e. washing the biofilm). Preliminary experiments using different substrates including glass beads and titanium discs were also unsuccessful, further suggesting substrate may not impact this ability. While it is possible that appropriate conditions have not yet been optimized to promote this biofilm formation, the current likely conclusion from this work may be that some

of these strains are simply unable to form strong biofilms, potentially lacking appropriate adhesion factors or ability to form an ECM.

4.3.5 – Phage ability to inhibit Staphylococcal biofilm formation varies based on host strain

Despite difficulties in forming strong biofilms with our strains, stable biofilm formation was achieved in *S. epidermidis* strains NRRL 41021 and ATCC 35984, and *S. succinus* strain ATCC 700337 to be used in the biofilm inhibition assay (Figure 11). This experiment observed a phages ability to prevent biofilm formation by *Staphylococcal* strains, which may be relevant to the potential application of phage as a preventative treatment applied during the surgical process, as antibiotic treatments are sometimes used in this way.

Notably, Pheter was utilized in all three experiments, where its activity differed between all three hosts, where resistant colonies were visualized representing greater resistance of *S. epidermidis* strains NRRL 41021 and ATCC 35984 in comparison to *S. succinus* 700337 where biofilms are near completely depleted and limited resistant colonies exist (Figure 11A, B, C). This observation is attributed to the fact that *S. succinus* species are generally not as virulent as *S. epidermidis*, and while they may form a physically more stable biofilm than some *S. epidermidis* species in the experiment, they are more easily susceptible to phage predation (54).

An additional discovery identified through this assay was the ability of the intended negative control phage Sachers in inhibiting the *S. succinus* biofilm, despite its inability to infect this host on plates (Figure 5, Figure 11C). This activity was attributed to potential depolymerase activity of *S. epidermidis* phages, where release of a depolymerase enzyme may disrupt layers of the *Staphylococcal* biofilm EPS matrix as it forms, thereby reducing biomass, while not necessarily selectively killing these cells (63).

4.3.6 – Phage ability to destroy Staphylococcal biofilms varies based on host strain

The biofilm destruction assay as intended to model a phage therapy application, where a phages efficacy in this experiment may suggest its efficacy against a PJI biofilm. In particular, the biofilms formed by NRRL 41021, were fragile, and in these assays were susceptible to flaking off the substrate upon phage or buffer addition. As this was an unavoidable step in carrying out the experiment, this strain was unable to be successfully used in a biofilm destruction assay. As discussed in Chapter 4.3.4, while more optimizations can be tested, including different substrates, it may be likely that because this strain is not a strong biofilm former, it is simply not ideal for carrying out this assay.

S. epidermidis ATCC 35984 formed a far more robust biofilm, that consequentially was highly resistant to phage predation (Figure 12A). Future attempts at this assay may choose to use higher concentration of phage, though this would only be achievable through PEG precipitation. As previously mentioned, this strain was known to have phage defence which may be more effective against predation when it in a biofilm state. Phage treatment could be further explored alongside an adjuvant treatment such as antibiotics, endolysin, or depolymerases in biofilm checkerboard assays.

Excitingly, *S. succinus* ATCC 700337 was susceptible to phage predation, however not to the same extent as observed in the biofilm inhibition assay (Figure 12B). Here, we see a notable difference between phage treated and untreated wells, suggesting that while these phages are effective, a far higher concentration may be required to fully destroy the biofilm. This panel allowed some confidence that our phages are effective against a pre-formed *Staphylococcal* biofilm, however more promising results would show a significant depletion in biofilm cells compared to the control.

These assays demonstrate that a pre-formed biofilm is far more difficult for *S. epidermidis* phages to destroy in contrast to inhibition of biofilm formation. Moreover, a robust biofilm, such as is formed by the more clinically relevant strain ATCC 35984, may be much more difficult to treat with these phages. The effect seen in the *S. succinus* biofilm demonstrates that biofilm depletion is possible, but altered conditions, higher concentrations of phage, or adjuvant treatments may be required to obtain promising effects. Additionally, the results of the biofilm destruction assay warrants consideration of if the biofilms formed in this assay are comparable to the *in vivo* biofilm formed in a PJI and should be used to predict the efficacy of a phage for phage therapy. To confirm this, a positive control phage could be used in these assays, such as the therapeutic phage used in the Ottawa Hospital PJI trial discussed in Chapter 1, to determine if this phage would be effective against our experimental conditions (1, 2).

Chapter 5 – Conclusion

Medical device-associated infections are the most common nosocomial infections and have devastating complications with lethal consequences. The most common culprit of these infections is *S. epidermidis*, where foreign implants offer the perfect stage for bacteria to form biofilms, becoming infectious and persisting throughout the body. As AMR rises among these already difficult to treat *Staphylococci* populations, alternative treatments are urgently needed. Bacteriophages are the natural predator to bacteria, and their abundance, diversity, and innate specificity makes them an optimal candidate for therapeutics. However, a major limitation to phage therapy is the challenge of finding lytic bacteriophages that infect the specific pathogenic bacteria causing the disease.

This study has established an Ottawa-based collection of bacteriophages that target *Staphylococcus epidermidis* that will help alleviate this bottleneck in phage therapy, allowing implementation of this treatment to become more efficient. In this study, we have successfully generated a collection of 79 bacteriophages infecting a diverse set of *S. epidermidis* strains, directly from skin swab samples, where 64 phages have been archived. We have successfully sequenced 77 total *Staphylococcal* bacteriophages and identify diverse phylogeny and clustering organization among the collection, with several phages appearing somewhat unique. Phage therapy-specific characterization efforts have identified a subset of six Cluster C and four Cluster D phages that exhibit a broad host range and strong lytic efficiency, recognizing them as candidates for therapeutic potential and requiring further study. Experimentation with biofilms recognizes weaknesses among several of the bacterial strains used in this study, where only one strain in the collection stands out with proficiency in forming biofilms. Despite this, several phages exhibit strong inhibitory activity against *S. epidermidis* and *S. succinus* biofilms. While our preliminary

results generate some confidence that our phages are active against pre-formed *Staphylococcal* biofilms, further optimization of this assay is required to identify conditions where these phages may better disrupt pre-formed biofilms. Moreover, future phage hunting efforts should be lead against strains with greater clinical relevance, to support the discovery of the most robust phages for this collection.

Future work will focus closely on the subset of phages of interest, where additional experimentation against biofilms and clinical isolate strains may be prioritized for confirming therapeutic efficiency of our phages. Additionally, complete genome sequencing and genome annotation must be performed to confirm that these phages lack lysogenic and virulence genes.

Ultimately, this project has created a baseline for future work on *Staphylococcal* phages, where our collection of 64 archived phages nearly meets the current availability of *S. epidermidis* phages worldwide. We hope that this project with inspire the creation of local biorepositories of therapeutic phages, thus that one day when an emergent phage therapy cases arises, these collections can be easily accessible and potential therapeutic phages can be tested.

References

1. ottawacitizen [Internet]. [cited 2025 Feb 1]. Ottawa doctor helping to bring back old treatment for new problems. Available from: https://ottawacitizen.com/news/ottawa-doctor-helping-to-bring-back-old-treatment-for-new-problems
2. Cammuso MT, Cook BWM, Cameron DW, Ryan S, Tamayo M, Peters MJ, et al. First Use of Phage Therapy in Canada for the Treatment of a Life-Threatening, Multidrug-Resistant *Staphylococcus epidermidis* Periprosthetic Joint Infection. Viruses. 2025 Aug 14;17(8):1118.
3. Dadi NCT, Radochová B, Vargová J, Bujdáková H. Impact of Healthcare-Associated Infections Connected to Medical Devices—An Update. Microorganisms. 2021 Nov 11;9(11):2332.
4. Ayoade F, Li D, Mabrouk A, Todd JR. Periprosthetic Joint Infection. In: StatPearls [Internet]. Treasure Island (FL): StatPearls Publishing; 2025 [cited 2025 Jan 27]. Available from:http://www.ncbi.nlm.nih.gov/books/NBK448131/
5. Bleß HH, Kip M, editors. White Paper on Joint Replacement: Status of Hip and Knee Arthroplasty Care in Germany [Internet]. Berlin (Germany): Springer; 2018. PMID: 31725204.
6. CJRR annual report: Hip and knee replacements in Canada, 2024–2025 | CIHI [Internet]. [cited 2026 Feb 20]. Available from: https://www.cihi.ca/en/cjrr-annual-report-hip-and-knee-replacements-in-canada-2024-2025
7. McMaster Arthroplasty Collaborative (MAC). Incidence and Predictors of Prosthetic Joint Infection Following Primary Total Knee Arthroplasty: A 15-Year Population-Based Cohort Study. J Arthroplasty. 2022 Feb;37(2):367-372.e1.
8. Patel R. Periprosthetic Joint Infection. N Engl . Med. 2023 Jan 18;388(3):251–62.
9. Licitra G. Etymologia: *Staphylococcus*. Emerg Infect Dis. 2013 Sep;19(9):1553.
10. Widerström M, Stegger M, Johansson A, Gurram BK, Larsen AR, Wallinder L, et al. Heterogeneity of *Staphylococcus epidermidis* in prosthetic joint infections: time to reevaluate microbiological criteria? Eur J Clin Microbiol Infect Dis. 2022;41(1):87–97. doi:10.1007/s10096-021-04352-w PubMed PMID: 34599708; PubMed Central PMCID: PMC8732909.
11. Lee E, Anjum F. *Staphylococcus epidermidis* Infection. In: StatPearls [Internet]. Treasure Island (FL): StatPearls Publishing; 2025 [cited 2025 Jan 27]. Available from: http://www.ncbi.nlm.nih.gov/books/NBK563240/
12. Kim HJ, Jo A, Jeon YJ, An S, Lee KM, Yoon SS, et al. Nasal commensal *Staphylococcus epidermidis* enhances interferon-λ-dependent immunity against influenza virus. Microbiome. 2019 May 30;7(1):80.
13. Fournière M, Latire T, Souak D, Feuilloley MGJ, Bedoux G. *Staphylococcus epidermidis* and *Cutibacterium acnes*: Two Major Sentinels of Skin Microbiota and the Influence of Cosmetics. Microorganisms. 2020 Nov 7;8(11):1752.
14. Zheng Y, Hunt RL, Villaruz AE, Fisher EL, Liu R, Liu Q, et al. Commensal *Staphylococcus epidermidis* contributes to skin barrier homeostasis by generating protective ceramides. Cell Host Microbe. 2022 Mar 9;30(3):301-313.e9.
15. Qi P, Gong F, Leng M, Wei Z. Beneficial perspective on *Staphylococcus epidermidis*: a crucial species for skin homeostasis and pathogen defense. Front Immunol. 2025 Oct 22;16:1674392.

16. Burke TL, Rupp ME, Fey PD. *Staphylococcus epidermidis*. Trends Microbiol. 2023 Jul 1;31(7):763–4. doi:10.1016/j.tim.2023.01.001
17. Fey PD, Olson ME. Current concepts in biofilm formation of *Staphylococcus epidermidis*. Future Microbiol. 2010 Jun;5(6):917–33.
18. Melo LDR, Pinto G, Oliveira F, Vilas-Boas D, Almeida C, Sillankorva S, et al. The Protective Effect of *Staphylococcus epidermidis* Biofilm Matrix against Phage Predation. Viruses. 2020 Sep 25;12(10):1076.
19. Nguyen HTT, Nguyen TH, Otto M. The *Staphylococcal* exopolysaccharide PIA – Biosynthesis and role in biofilm formation, colonization, and infection. Comput Struct Biotechnol J. 2020 Nov 4;18:3324–34.
20. Otto M. *Staphylococcus epidermidis* – the "accidental" pathogen. Nat Rev Microbiol. 2009 Aug;7(8):555–67. doi:10.1038/nrmicro2182 PubMed PMID: 19609257; PubMed Central PMCID: PMC2807625.
21. Herman P, El-Kirat-Chatel S, Beaussart A, Geoghegan JA, Foster TJ, Dufrêne YF. The binding force of the *Staphylococcal* adhesin SdrG is remarkably strong. Mol Microbiol. 2014 Jul;93(2):356–68. doi:10.1111/mmi.12663 PubMed PMID: 24898289.
22. Mack D, Fischer W, Krokotsch A, Leopold K, Hartmann R, Egge H, et al. The intercellular adhesin involved in biofilm accumulation of *Staphylococcus epidermidis* is a linear beta-1,6-linked glucosaminoglycan: purification and structural analysis. J Bacteriol. 1996 Jan;178(1):175–83. doi:10.1128/jb.178.1.175-183.1996 PubMed PMID: 8550413; PubMed Central PMCID: PMC177636.
23. AL-Ishaq R, Armstrong J, Gregory M, O'Hara M, Phiri K, Harris LG, et al. Effects of polysaccharide intercellular adhesin (PIA) in an *ex vivo* model of whole blood killing and in prosthetic joint infection (PJI): A role for C5a. Int J Med Microbiol. 2015 Dec 1;305(8):948–56. doi:10.1016/j.ijmm.2015.08.005
24. Antimicrobial resistance [Internet]. [cited 2025 Feb 5]. Available from: https://www.who.int/news-room/fact-sheets/detail/antimicrobial-resistance
25. Naghavi M, Vollset SE, Ikuta KS, Swetschinski LR, Gray AP, Wool EE, et al. Global burden of bacterial antimicrobial resistance 1990–2021: a systematic analysis with forecasts to 2050. The Lancet. 2024 Sep 28;404(10459):1199–226.
26. Beck C, Krusche J, Elsherbini AMA, Du X, Peschel A. Phage susceptibility determinants of the opportunistic pathogen *Staphylococcus epidermidis*. Curr Opin Microbiol. 2024 Apr 1;78:102434.
27. Strathdee SA, Hatfull GF, Mutalik VK, Schooley RT. Phage therapy: From biological mechanisms to future directions. Cell. 2023 Jan 5;186(1):17–31.
28. Lin DM, Koskella B, Lin HC. Phage therapy: An alternative to antibiotics in the age of multi-drug resistance. World J Gastrointest Pharmacol Ther. 2017 Aug 6;8(3):162–73.
29. Leprince A, Mahillon J. Phage Adsorption to Gram-Positive Bacteria. Viruses. 2023 Jan 10;15(1):196.
30. Degroux S, Effantin G, Linares R, Schoehn G, Breyton C. Deciphering Bacteriophage T5 Host Recognition Mechanism and Infection Trigger. J Virol. 97(3):e01584-22. 1.
31. Ptashne M. A genetic switch: phage lambda revisited. 3rd Edition. Cold Spring Harb Lab Press; 2004.
32. Caudovirales - an overview | ScienceDirect Topics [Internet]. [cited 2025 Jan 30]. Available from: https://www.sciencedirect.com/topics/biochemistry-genetics-and-molecular-biology/caudovirales.

33. Current ICTV Taxonomy Release | ICTV [Internet]. [cited 2026 Mar 26]. Available from: https://ictv.global/taxonomy
34. Oliveira H, Sampaio M, Melo LDR, Dias O, Pope WH, Hatfull GF, et al. *Staphylococci* phages display vast genomic diversity and evolutionary relationships. BMC Genomics. 2019 May 9;20(1):357.
35. Andrews T, Hoyer JS, Ficken K, Fey PD, Duffy S, Boyd JM. A Transducing Bacteriophage Infecting *Staphylococcus epidermidis* Contributes to the Expansion of a Novel Siphovirus Genus and Implies the Genus Is Inappropriate for Phage Therapy. mSphere. 8(3):e00524-22. doi:10.1128/msphere.00524-22 PubMed PMID: 37017574; PubMed Central PMCID: PMC10286716.
36. Štrancar V, Marušić M, Tušar J, Praček N, Kolenc M, Šuster K, et al. Isolation and in vitro characterization of novel *S. epidermidis* phages for therapeutic applications. Front Cell Infect Microbiol. 2023;13:1169135.
37. Pirnay JP, Blasdel BG, Bretaudeau L, Buckling A, Chanishvili N, Clark JR, et al. Quality and safety requirements for sustainable phage therapy products. Pharm Res. 2015 Jul;32(7):2173–9.
38. Favaro A. CTVNews [Internet]. 2023 [cited 2026 Mar 15]. First Canadian trial successfully uses phage therapy to stop life-threatening UTI caused by superbug. Available from: https://www.ctvnews.ca/health/article/first-canadian-trial-successfully-uses-phage-therapy-to-stop-life-threatening-uti-caused-by-superbug/
39. Canada PHA of. Pan-Canadian Action Plan on Antimicrobial Resistance: Year 1 Progress Report (June 2023 to May 2024) [education and awareness] [Internet]. 2024 [cited 2026 Mar 16]. Available from: https://www.canada.ca/en/public-health/services/publications/drugs-health-products/pan-canadian-action-plan-antimicrobial-resistance-year-1-progress-report-2023-2024.html
40. Lopes MS, Silva MD, Azeredo J, Melo LDR. Coagulase-Negative *Staphylococci* phages panorama: Genomic diversity and *in vitro* studies for a therapeutic use. Microbiol Res. 2025 Jan 1;290:127944.
41. Hatfull GF. Mycobacteriophages. Microbiol Spectr. 6(5): 10.1128/microbiolspec.gpp3-0026-2018 PubMed PMID: 30291704; PubMed Central PMCID: PMC6282025.
42. SEA-Phages Discovery Guide [Internet]. [cited 2025 Jan 27]. Available from: https://seaphagesphagediscoveryguide.helpdocsonline.com/home
43. Valente LG, Pitton M, Fürholz M, Oberhaensli S, Bruggmann R, Leib SL, et al. Isolation and characterization of bacteriophages from the human skin microbiome that infect *Staphylococcus epidermidis*. FEMS Microbes. 2021;2:xtab003. doi:10.1093/femsmc/xtab003 PubMed PMID: 37334235; PubMed Central PMCID: PMC10117716.
44. Fox B, Chahal J, Lypaczewski P. DNA extraction free whole genome sequencing of bacteriophage genomes from a single plaque [Internet]. bioRxiv; 2025 [cited 2026 Mar 16]. p. 2025.10.21.683754. Available from: https://www.biorxiv.org/content/10.1101/2025.10.21.683754v1 doi:10.1101/2025.10.21.683754
45. Wang RH, Yang S, Liu Z, Zhang Y, Wang X, Xu Z, et al. PhageScope: a well-annotated bacteriophage database with automatic analyses and visualizations. Nucleic Acids Res. 2023 Oct 30;52(D1):D756–61. doi:10.1093/nar/gkad979 PubMed PMID: 37904614; PubMed Central PMCID: PMC10767790.

46. Letunic I, Bork P. Interactive Tree of Life (iTOL) v6. Nucleic Acids Research. 2024 Jul 5;52(W1):W78–82. doi:10.1093/nar/gkae268
47. Kawasaki K, Kamagata Y. Phosphate-Catalyzed Hydrogen Peroxide Formation from Agar, Gellan, and κ-Carrageenan and Recovery of Microbial Cultivability via Catalase and Pyruvate. Appl Environ Microbiol. 2017 Nov 1;83(21):e01366-17. doi:10.1128/AEM.01366-17 PubMed PMID: 28821549; PubMed Central PMCID: PMC5648910.
48. Hyman P. Phages for Phage Therapy: Isolation, Characterization, and Host Range Breadth. Pharmaceuticals (Basel). 2019 Mar 11;12(1):35. doi:10.3390/ph12010035 PubMed PMID: 30862020; PubMed Central PMCID: PMC6469166.
49. Welcome to the ARS Culture Collection (NRRL) | ARS Culture Collection [Internet]. [cited 2025 Feb 1]. Available from: https://nrrl.ncaur.usda.gov/https://www.atcc.org [Internet]. [cited 2026 Mar 22].
50. ATCC: The Global Bioresource Center. Available from: https://www.atcc.org/
51. The Actinobacteriophage Database | Phage List [Internet]. [cited 2026 Mar 26]. Available from: https://phagesdb.org/phages/
52. https://www.atcc.org [Internet]. [cited 2026 Mar 26]. *Staphylococcus epidermidis* (Winslow and Winslow) Evans - 35984 | ATCC. Available from: https://www.atcc.org/products/35984
53. Marraffini LA, Sontheimer EJ. CRISPR Interference Limits Horizontal Gene Transfer in *Staphylococci* by Targeting DNA. Science. 2008 Dec 19;322(5909):1843–5. doi:10.1126/science.1165771 PubMed PMID: 19095942; PubMed Central PMCID: PMC2695655.
54. *Staphylococcus succinus* subsp. succinus Lambert et al. - 700337 | ATCC [Internet]. [cited 2026 Mar 26]. Available from: https://www.atcc.org/products/700337
55. Coombs D. T4 tail structure and function. 1994;259–81.
56. Nucleotide BLAST: Search nucleotide databases using a nucleotide query [Internet]. [cited 2025 Feb 1]. Available from: https://blast.ncbi.nlm.nih.gov/Blast.cgi?PROGRAM=blastn&PAGE_TYPE=BlastSearch&LINK_LOC=blasthome
57. Abedon ST. Lysis from without. Bacteriophage. 2011;1(1):46–9. doi:10.4161/bact.1.1.13980 PubMed PMID: 21687534; PubMed Central PMCID: PMC3109453.
58. Ma Y, Chen M, Jones JE, Ritts AC, Yu Q, Sun H. Inhibition of *Staphylococcus epidermidis* Biofilm by Trimethylsilane Plasma Coating. Antimicrob Agents Chemother. 2012 Nov;56(11):5923–37. doi:10.1128/AAC.01739-12 PubMed PMID: 22964248; PubMed Central PMCID: PMC3486604.
59. Kwasny SM, Opperman TJ. Static biofilm cultures of Gram-positive pathogens grown in a microtiter format used for anti-biofilm drug discovery. Curr Protoc Pharmacol. 2010 Sep 1;50:13A.8.1-13A.8.23. doi:10.1002/0471141755.ph13a08s50 PubMed PMID: 22294365; PubMed Central PMCID: PMC3272335.

60. Taha M, Kalab M, Yi QL, Landry C, Greco-Stewart V, Brassinga AK, et al. Biofilm-forming skin microflora bacteria are resistant to the bactericidal action of disinfectants used during blood donation. Transfusion. 2014 Nov;54(11):2974–82. doi:10.1111/trf.12728 PubMed PMID: 24889094.
61. Ferriol-González C, Concha-Eloko R, Bernabéu-Gimeno M, Fernández-Cuenca F, Cañada-García JE, García-Cobos S, Sanjuán R, Domingo-Calap P. Targeted phage hunting to specific *Klebsiella pneumoniae* clinical isolates is an efficient antibiotic resistance and infection control strategy. Microbiol Spectr. 2024 Aug 28. 12:e00254-24. https://doi.org/10.1128/spectrum.00254-24
62. Cater K, Dandu VS, Bari SMN, Lackey K, Everett GFK, Hatoum-Aslan A. A Novel *Staphylococcus* Podophage Encodes a Unique Lysin with Unusual Modular Design. mSphere. 2017 Mar 22;2(2):e00040-17. doi:10.1128/mSphere.00040-17 PubMed PMID: 28357414; PubMed Central PMCID: PMC5362749.
63. Abedon ST, Danis-Wlodarczyk KM, Wozniak DJ, Sullivan MB. Improving Phage-Biofilm In Vitro Experimentation. Viruses. 2021 Jun 19;13(6):1175. doi:10.3390/v13061175 PubMed PMID: 34205417; PubMed Central PMCID: PMC8234374.